A State-of-the-Art Survey on Reconfigurable Intelligent Surface-Assisted Non-Orthogonal Multiple Access Networks

This article provides an overview of the recent progress on the synergistic integration of reconfigurable intelligent surfaces and non-orthogonal multiple access schemes.

By Zhiguo Ding, *Fellow IEEE*, Lu Lv, *Member IEEE*, Fang Fang, *Member IEEE*, Octavia A. Dobre, *Fellow IEEE*, George K. Karagiannidis, *Fellow IEEE*, Naofal Al-Dhahir, *Fellow IEEE*, Robert Schober, *Fellow IEEE*, and H. Vincent Poor, *Life Fellow IEEE*

Manuscript received 10 August 2021; revised 13 January 2022; accepted 17 April 2022. Date of publication 23 May 2022; date of current version 19 September 2022. The work of Zhiguo Ding was supported in part by H2020-MSCA-RISE-2020 under Grant 101006411 and in part by the Friedrich Wilhelm Bessel Research Prize from the Alexander von Humboldt Foundation. The work of Lu Lv was supported in part by the National Natural Science Foundation of China under Grant 61901313 and in part by the China Postdoctoral Science Foundation under Grant BX20190264 and Grant 2019M650258. The work of Robert Schober was supported in part by the BMBF Project 6G-RIC under Grant 16KISK023 and in part by the German Science Foundation under Grant SCHO 831/15-1. The work of H. Vincent Poor was supported by the U.S. National Science Foundation under Grant CCF-1908308. The work of Naofal Al-Dhahir was supported in part by the Qualcomm Faculty Award and in part by the Erik Jonsson Distinguished Professorship. *(Corresponding author: Zhiguo Ding.)*

Zhiguo Ding is with the Department of Electrical and Computer Engineering, Princeton University, Princeton, NJ 08544 USA, and also with the School of Electrical and Electronic Engineering, The University of Manchester, Manchester M13 9PL, U.K. (e-mail: zhiguo.ding@manchester.ac.uk).

Lu Lv is with the State Key Laboratory of Integrated Services Networks, Xidian University, Xi'an 710071, China (e-mail: lulv@xidian.edu.cn).

Fang Fang is with the Department of Electrical and Computer Engineering and the Department of Computer Science, Western University, London, ON N6A 3K7, Canada (e-mail: fang.fang@uwo.ca).

Octavia A. Dobre is with the Faculty of Engineering and Applied Science, Memorial University, St. John's, NL A1B 3X5, Canada (e-mail: odobre@mun.ca).

George K. Karagiannidis is with the Wireless Communications and Information Processing (WCIP) Group, Department of Electrical and Computer Engineering, Aristotle University of Thessaloniki, 54 124 Thessaloniki, Greece (e-mail: geokarag@auth.gr).

Naofal Al-Dhahir is with the Department of Electrical and Computer Engineering, The University of Texas at Dallas, Richardson, TX 75080 USA (e-mail: aldhahir@utdallas.edu).

Robert Schober is with the Institute for Digital Communications, Friedrich-Alexander-University Erlangen-Nurnberg (FAU), 91058 Erlangen, Germany (e-mail: robert.schober@fau.de).

H. Vincent Poor is with the Department of Electrical and Computer Engineering, Princeton University, Princeton, NJ 08544 USA (e-mail: poor@princeton.edu).

Digital Object Identifier 10.1109/JPROC.2022.3174140

ABSTRACT | Reconfigurable intelligent surfaces (RISs) and nonorthogonal multiple access (NOMA) have been recognized as key enabling techniques for the envisioned sixth generation (6G) of mobile communication networks. The key feature of RISs is to intelligently reconfigure the wireless propagation environment, which was once considered to be fixed and untunable. The key idea of NOMA is to utilize users' dynamic channel conditions to improve spectral efficiency and user fairness. Naturally, the two communication techniques are complementary to each other and can be integrated to cope with the challenging requirements envisioned for 6G mobile networks. This survey provides a comprehensive overview of the recent progress on the synergistic integration of RISs and NOMA. In particular, the basics of both techniques are introduced first, and then, the fundamentals of RIS-NOMA are discussed for two communication scenarios with different transceiver capabilities. Resource allocation is of paramount importance for the success of RIS-assisted NOMA networks, and various approaches, including artificial intelligence (AI)-empowered designs, are introduced. Security provisioning in RIS-NOMA networks is also discussed as wireless networks are prone to security attacks due to the nature of the shared wireless medium. Finally, the survey is concluded with detailed discussions of the challenges arising in the practical implementation of RIS-NOMA, future research directions, and emerging applications.

KEYWORDS | Artificial intelligence (AI); multi-input multi-output (MIMO); nonorthogonal multiple access (NOMA); reconfigurable intelligent surface (RIS); resource allocation; wireless security.

I. INTRODUCTION

With the rapid rollout of fifth generation (5G) mobile networks, the focus of the research community is currently shifting toward the design of beyond 5G (B5G) and sixth generation (6G) networks [1]–[4]. Notably, the envisioned performance metrics of B5G and 6G are much more demanding than those for the previous generations of wireless systems. For example, B5G and 6G systems are expected to support users with extremely diverse data rate requirements, where an augmented reality (AR) or virtual reality (VR) user might demand a peak data rate of several terabits per second (Tbps), but an Internet-of-Things (IoT) node could be served with a data rate in the kilobit-per-second range. Another example is that the connection density supported in B5G and 6G systems is expected to be 100 times higher than that of 5G, e.g., more than 10^7 devices/km^2 may be connected [1]. To meet these demanding and diverse requirements for B5G and 6G, more intelligent techniques that can efficiently increase transmission reliability, improve system throughput, and support massive connectivity are needed.

Reconfigurable intelligent surfaces (RISs) and nonorthogonal multiple access (NOMA) have been recognized as two very promising communication techniques to meet the aforementioned challenges for the design of B5G and 6G systems. On the one hand, an RIS can intelligently reconfigure a mobile user's propagation environment, which ensures that the user's data rate and reception reliability can be significantly improved [5]–[14]. Note that these performance improvements are realized in a low-cost, energy-efficient, and spectrally efficient manner since no additional spectrum needs to be acquired and the success of RISs is due to their ability to create favorable radio propagation conditions. On the other hand, NOMA can effectively increase spectral efficiency, support massive connectivity, improve user fairness, and reduce transmission latency, by encouraging dynamic spectrum sharing among mobile users and opportunistically exploiting their heterogeneous channel conditions and quality-of-service (QoS) requirements [15]–[23].

Naturally, these two important enabling technologies are complementary to each other, where the use of NOMA can improve the spectral efficiency and connectivity of RIS systems and the use of RISs ensures that the users' propagation environments can be effectively and intelligently customized for the implementation of NOMA. In particular, many forms of NOMA have been developed to encourage dynamic spectrum sharing among mobile users by opportunistically exploiting the users' heterogeneous channel conditions. Conventionally, a user's channel conditions are viewed as a type of fixed and nontunable phenomenon that is solely determined by the user's propagation environment. Therefore, if the users' channel conditions are not ideal for the application of NOMA, e.g., when the users have similar channel conditions, the performance gain of NOMA over conventional orthogonal multiple access (OMA) can be quite limited. RISs enable a paradigm shift for the design of intelligent NOMA since the use of an RIS ensures that the propagation environment can be effectively and intelligently customized for the needs of NOMA.

This article provides a comprehensive overview of the opportunities and challenges that arise in connection with the integration of RISs and NOMA in the envisioned next-generation mobile networks. In particular, we will focus on the following aspects.

1) The basics of the two considered communication techniques, namely, RISs and NOMA, are reviewed first. In particular, the capability of NOMA to facilitate spectrum sharing among mobile users to improve spectral efficiency is described, and the key idea behind RISs, i.e., reconfiguration of the users' propagation environment, is illustrated.
2) Then, the fundamentals of RIS-NOMA are presented, where the benefits of the integration of RIS and NOMA are unveiled. Furthermore, the quasi-degradation criterion is used as a metric to illustrate how the use of RIS guarantees that NOMA can realize the same performance as dirty paper coding (DPC), but with lower computational complexity.
3) Dynamic resource allocation is crucial for realizing the performance gains enabled by RIS-NOMA and is reviewed. In particular, RIS-NOMA offers additional degrees of freedom (DoFs) in the spatial, frequency, and time domains. We will show how these DoFs can be effectively exploited to improve the system performance by applying matching and game-theoretic techniques. Artificial intelligence (AI)/machine learning (ML)-empowered RIS-NOMA is presented. In particular, the benefits of using AI tools for realizing long-term performance gains in RIS-NOMA networks are illustrated, where conventional optimization tools serve as benchmarks.
4) Security provisioning via RIS-NOMA is also covered in this survey. The application of RIS-NOMA to enhance physical layer security with respect to passive eavesdropping is studied first, where the impact of using an RIS on the secrecy performance is illustrated. Then, the application of RIS-NOMA to covert communications is investigated.
5) While RIS-NOMA can offer various performance gains, its practical implementation faces many challenges, which are discussed here as well. In particular, the design of channel estimation schemes for RIS-NOMA networks is considered. This is a challenging problem, due to the passive nature of RIS arrays and the multiuser nature of NOMA. Low-complexity solutions for practical deployment of RISs in NOMA networks are introduced.
6) RIS-NOMA has widespread applications in various communication network architectures, which are presented in this survey. In particular, the exploitation of

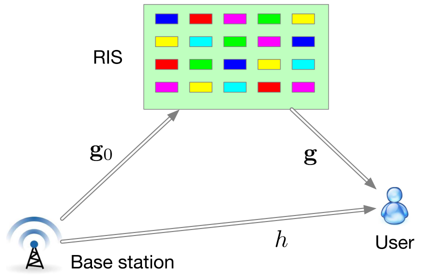

Fig. 1. ***Illustration example for RIS transmission.***

unmanned aerial vehicles (UAVs) equipped with RISs to support aerial radio access networks is described. Other applications of RIS-NOMA, such as mobile edge computing (MEC) and wireless power transfer (WPT), are presented as well.

The remainder of this survey is organized as follows. In Section II, the basics of RIS and NOMA are reviewed, and the fundamentals of RIS-NOMA are elaborated in Section III. Existing resource allocation approaches for RIS-NOMA are surveyed in Section IV, where AI-empowered approaches are also discussed. Security provisioning and the practical implementation of RIS-NOMA are considered in Sections V and VI, respectively. The survey is concluded with a discussion of various future research directions and emerging applications for RIS-NOMA.

II. BASICS OF RISs AND NOMA

In this section, the basics of the two considered communication techniques, RISs and NOMA, are briefly reviewed.

A. RISs

Unlike conventional information transmitters and receivers, RISs themselves do not have any information to send but are deployed to assist information transceivers [5]–[7]. The basic idea of RIS systems can be illustrated by using the simple example shown in Fig. 1, where a single-antenna base station (BS) communicates with a single-antenna user via an RIS equipped with N reflecting elements. For this illustrative example, the signal received by the user can be expressed as follows:

$$y = (h + \mathbf{g}_0^H \boldsymbol{\Theta} \mathbf{g})s + w \tag{1}$$

where s denotes the information symbol, h denotes the channel gain between the BS and the user, $\boldsymbol{\Theta}$ is an $N \times N$ diagonal matrix, $\mathbf{g}_0$ denotes the channel vector between the RIS and the user, $\mathbf{g}$ denotes the channel vector between the BS and the RIS, and w denotes the noise. In the RIS literature, $\boldsymbol{\Theta}$ is termed the phase shifting matrix since the RIS does not change the amplitudes of the reflected signals but alters their phases only [8]–[10]. Denote the ith main diagonal element of $\boldsymbol{\Theta}$ by $e^{j\theta_i}$, where θ_i is the phase shift caused by the ith reflecting element of the RIS.

In Fig. 2, the performance achieved for the considered RIS-assisted single-user scenario is illustrated by using the outage rate as the performance metric. In particular, the outage rate is defined as follows: $R[1 - P(\log(1 + \rho|\mathbf{g}_0^H \boldsymbol{\Theta}\mathbf{g}|^2) < R)]$, where $P(\log(1 + \rho|\mathbf{g}_0^H \boldsymbol{\Theta}\mathbf{g}|^2) < R)$ denotes the probability of the outage event $(\log(1 + \rho|\mathbf{g}_0^H \boldsymbol{\Theta}\mathbf{g}|^2) < R)$, ρ denotes the transmit signal-to-noise ratio (SNR), and R denotes the user's target data rate. For the considered simple example, the phase shifts are obtained by first generating N sets of random phases and selecting the best set yielding the largest data rate. Note that finding the optimal phase shifts is the key step for the design of RIS systems, and the design principles for optimizing the RIS phase shifts will be provided in detail in the following.

As can be observed from Fig. 2, the use of an RIS with $N = 20$ reflecting elements can already offer a significant performance gain over the scheme without an RIS. For example, with a transmit power of 5 dBm, the data rate achieved by the scheme without an RIS is 0.6 bit per channel use (BPCU), while the RIS-assisted scheme can realize a data rate of 1.7 BPCU in Case 2. By increasing the number of RIS reflecting elements, the performance gain achieved with the RIS can be further improved. For example, for Case 2 and a transmit power of 5 dBm, Fig. 2 shows that an RIS with $N = 50$ reflecting elements yields a data rate of 3.3 BPCU, which is more than five times the data rate compared to the scheme without an RIS. It is also interesting to observe that the performance of the RIS-assisted system is affected by the location of the RIS,

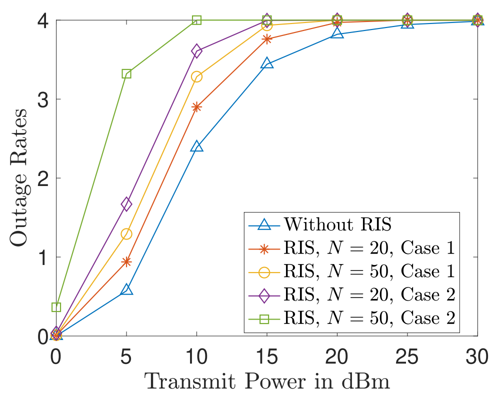

Fig. 2. ***Illustration of the performance of RIS transmission. The distance between the BS and the user is 30 m. For Case 1, the RIS is located at a vertex of an equilateral triangle whose other two vertices are the user and the BS, and for Case 2, the RIS is located at the center of the aforementioned equilateral triangle. Both small-scale Ricean fading and large-scale path loss are considered. The path loss is modeled by (c_0/d^α), where α denotes the path loss exponent and c_0 denotes the reference power gain at the distance of 1 m. The path loss exponent for the channel between the BS and the user is 4, i.e., the direct link suffers severe blockage, the path loss exponents for the channels related to the RIS are 2.2, and $c_0 = -30$ dB [24]–[26]. The user's target data rate is 4 BPCU. The noise power is -90 dBm.***

where a more detailed discussion on how to optimize the deployment of RISs will be provided in Section VI.

B. NOMA

As a multiple access technique that allows multiple users to concurrently use scarce bandwidth resources, NOMA is fundamentally different from conventional OMA, which permits users to only individually occupy orthogonal bandwidth resource blocks. Instead, the key principle of NOMA transmission is to encourage spectrum sharing among users, e.g., multiple users are allowed to be served at the same time and frequency [15], [16]. The key idea behind NOMA can be illustrated based on power-domain NOMA,[1] which encourages users with different channel conditions to share the spectrum [32], [33]. The success of power-domain NOMA is based on its capability to efficiently exploit the users' dynamic channel conditions, as explained in the following.

Consider a simple downlink scenario with one BS and two users, as shown in Fig. 3(a), where each node is equipped with a single antenna. Assume that user 1 has a weak channel gain, denoted by h_1, and user 2 has a strong channel gain, denoted by h_2, i.e., $|h_1|^2 \leq |h_2|^2$. In conventional OMA, each user occupies a different orthogonal bandwidth resource, such as a time slot, whereas in NOMA, both users are served simultaneously in the same resource. In particular, the BS sends a superimposed signal, i.e., $x = \alpha_1 s_1 + \alpha_2 s_2$, where s_i denotes user i's signal and α_i denotes the power allocation coefficient for user i's signal. Unlike conventional power allocation polices which allocate more power to users with strong channel conditions, NOMA allocates more power to the weak user, i.e., $\alpha_1 \geq \alpha_2$, in order to ensure that both users are connected. The two users adopt different detection strategies, depending on their channel conditions. As the weak user, user 1 treats user 2's signal as noise and tries to directly decode its own message with a rate of $\log(1 + (|h_1|^2\alpha_1^2/|h_1|^2\alpha_2^2 + (1/\rho)))$. As the strong user, user 2 applies successive interference cancellation (SIC), i.e., it decodes user 1's signal first with a rate of $\log(1+(|h_2|^2\alpha_1^2/|h_2|^2\alpha_2^2+(1/\rho)))$. If the first stage of SIC is carried out successfully, user 2 can remove user 1's signal and decode its own signal with a rate of $\log(1+\rho|h_2|^2\alpha_2^2)$. On the other hand, the data rates achieved by OMA are given by $(1/2)\log(1 + |h_i|^2)$, for $i \in \{1, 2\}$, where the factor $(1/2)$ is due to the fact that each user can use the resource half of the time only.

In Fig. 3(b), the outage sum rate is used as a metric for performance evaluation, where the outage sum rate is defined as $R_1(1 - P_1) + R_2(1 - P_2)$, R_i denotes the user i's target data rate

$$P_1 = P\left(\log\left(1 + \frac{|h_1|^2\alpha_1^2}{|h_1|^2\alpha_2^2 + \frac{1}{\rho}}\right) < R_1\right) \qquad (2)$$

[1]We note that there are various forms of NOMA, which exploit not only the users' different channel conditions but also the users' heterogeneous QoS requirements [15], [16], [27]–[31].

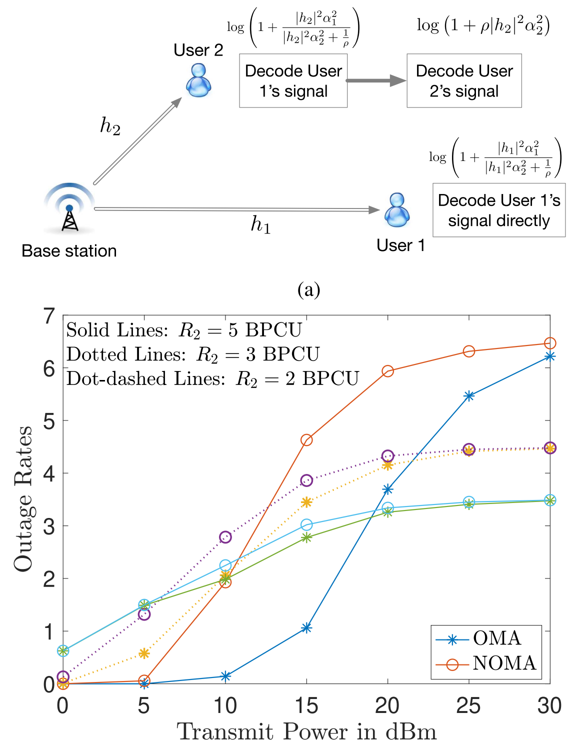

Fig. 3. *Illustrative example for NOMA. The distance between the BS and user 1 is 50 m, and the distance between the BS and user 2 is 20 m. Both small-scale Ricean fading and large-scale path loss are considered, with a path loss exponent of 4. User 1's target data rate is $R_1 = 1.5$ BPCU, and user 2's target date rate is denoted by R_2. The other simulation parameters are the same as the ones used for Fig. 2. (a) Two-user NOMA example. (b) Outage sum rates achieved by NOMA.*

and

$$P_2 = 1 - P\left(\log\left(1 + \frac{|h_2|^2\alpha_1^2}{|h_2|^2\alpha_2^2 + \frac{1}{\rho}}\right) > R_1, \right. \\ \left. \log\left(1 + \rho|h_2|^2\alpha_2^2\right) > R_2\right). \qquad (3)$$

As can be observed from the figure, NOMA can yield a significant performance gain over OMA. For example, for $R_2 = 5$ BPCU and a transmit power of 15 dBm, the outage sum rate realized by NOMA is 4.6 BPCU, which is more than four times the data rate achieved by OMA. An important observation from the figure is that the performance gain of NOMA over OMA diminishes when the two users have similar target data rates. Thus, NOMA cannot only exploit the users' heterogeneous channel conditions but also other user heterogeneities, such as users' different mobility profiles and QoS requirements [15], [16], [27]–[31].

III. FUNDAMENTALS OF RIS-NOMA

Although the concepts of RISs and NOMA have been developed separately in the literature, the two communication

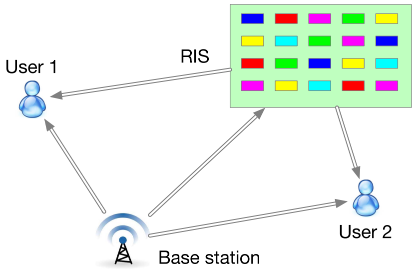

Fig. 4. *Illustration for a two-user RIS-NOMA network.*

techniques are naturally complementary to each other. In this section, the fundamentals of RIS-NOMA are described and the benefits of RIS-NOMA are illustrated based on a simple two-user example. The two users are denoted by users 1 and 2, as shown in Fig. 4. In particular, two scenarios, namely, single-input–single-output (SISO) and multiple-input–single-output (MISO) transmission, are studied in Sections III-A and III-B, respectively.

A. SISO-RIS-NOMA

Consider an SISO scenario, where each node in the network is equipped with a single antenna. For this simple scenario, the use of NOMA is clearly motivated since it can ensure that the two users are served simultaneously, whereas RIS-OMA can support only a single user at a time. The application of RISs to NOMA is motivated in the following.

Without RIS, the performance gain of NOMA over OMA is critically depending on the two users' channels, denoted by h_1 and h_2, as shown in the following. If power-domain NOMA is used and the users' channels are the same, the achievable sum rate is given by

$$\log\left(1+\frac{|h_1|^2\alpha_1^2}{|h_1|^2\alpha_2^2+\frac{1}{\rho}}\right)+\log\left(1+\rho|h_2|^2\alpha_2^2\right) = \log\left(1+\rho|h_2|^2\right) \quad (4)$$

which is the same as the sum rate achieved by OMA.

Conventionally, the users' channel conditions are viewed as being fixed and solely determined by the users' propagation environment. However, the use of RISs opens up opportunities for intelligently reconfiguring the users' propagation environment in order to facilitate the application of NOMA, which can lead to significant performance gains of NOMA over OMA. In particular, with an RIS, the two users' effective channel gains are given by [5], [6]

$$\tilde{h}_i = h_i + \mathbf{g}^H\boldsymbol{\Theta}\mathbf{g}_i, \quad i\in\{1,2\} \quad (5)$$

where $\mathbf{g}_i$ denotes the channel vector between the RIS and user i and $\mathbf{g}$ and $\boldsymbol{\Theta}$ are defined in Section II. By intelligently tuning $\boldsymbol{\Theta}$, RIS-NOMA can introduce more DoFs for system design. This can be exploited to not only generate a significant difference in the users' channel gains but also to customize the users' effective channel gains according to the users' QoS requirements, as shown in Fig. 5, where it is assumed that $h_1 = h_2$. As discussed before, this situation is not suitable for the application of power-domain NOMA. As can be observed from the figure, the use of RISs can effectively generate sufficient differences between the users' effective channel gains. For example, for Case 1 shown in Fig. 5, user 1's channel gain is almost two times larger than user 2's channel gain, which means that user 1 can act as the strong user and user 2 can act as the weak user in power-domain NOMA. If user 2 has a more stringent target data rate and needs to be treated as the strong user, Fig. 5 shows that this can be realized by simply adjusting $\boldsymbol{\Theta}$.

The fundamentals of SISO-RIS-NOMA have been thoroughly analyzed in the literature from various perspectives. For example, in [34], the energy efficiency (EE) of downlink SISO-RIS-NOMA has been studied, where SISO-RIS-OMA has been used as a benchmark. As shown in [34], when the users have different data rate requirements, the use of RIS-NOMA can realize a reduction in the transmit power by almost a factor of 2, even if the users have similar channel conditions, whereas the performance gain of RIS-NOMA diminishes if the users have similar target data rate requirements. Another performance criterion used in the literature is reception reliability, where the works in [35] and [36] demonstrate that downlink SISO-RIS-NOMA can efficiently utilize the spatial DoFs to improve the reception reliability compared to RIS-OMA. In particular, the use of SISO-RIS-NOMA can ensure that the diversity gain achieved by each user in the system is

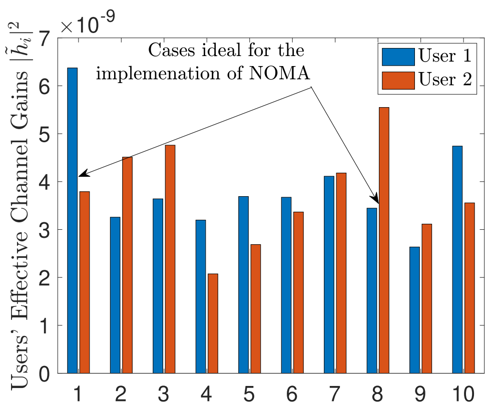

Fig. 5. *Illustration of the benefit of using SISO-RIS-NOMA for $N = 100$. The BS and the two users are located at the vertices of an equilateral triangle with side length $d = 30$ m, and the RIS is located at the center of the triangle. For illustrative purposes, small-scale fading is omitted for the users' direct channels to the BS such that the users have the same channel gains, $h_1 = h_2$ because their distances to the BS are the same. The other simulation parameters are the same as the ones used for Fig. 2. The ten cases are generated by using ten random phase shift configurations.*

proportional to the number of reflecting elements of the RIS, even though the multiple users share the same bandwidth resource. The application of SISO-RIS-NOMA for uplink transmission has been studied in [37], where the sum rate is used as the metric. In particular, Zeng *et al.* [37] showed that the use of RIS-NOMA can yield significant performance improvements when the number of RIS elements is large. Another important finding in [37] is that the use of NOMA is particularly useful in crowded scenarios, e.g., a performance gain of 5 BPCU over OMA is achievable for the two-user case, and it can be increased to 8 BPCU when there are six users.

B. MISO-RIS-NOMA

Consider an MISO scenario, where the BS is equipped with multiple antennas and each user has a single antenna. The benefit of the integration of RISs and NOMA can be clearly illustrated by using the quasi-degradation criterion, an insightful condition under which the use of MISO-NOMA results in the same performance as DPC but with less complexity [38], [39].

The quasi-degradation criterion can be illustrated by considering a simple two-user downlink scenario, where the BS has two antennas, and each user has a single antenna. The two users' channel vectors are denoted by $\mathbf{h}_i$ and assumed to be real-valued vectors. Furthermore, assume that user 1's channel vector is fixed, i.e., $\mathbf{h}_1 = \begin{bmatrix}1 & 1\end{bmatrix}^T$. The shaded region shown in Fig. 6(a) is obtained by highlighting the nonquasi-degradation (NQD) region, i.e., those realizations of $\mathbf{h}_2$ that do not meet the quasi-degradation condition [38], [39]. For example, Case 1 shown in the figure, i.e., the two users' channel vectors are almost aligned, is in the quasi-degradation region. This is an ideal case for using NOMA since the users' channel vectors occupy a single spatial direction and one beam can be used to serve both users simultaneously. Case 2, i.e., the two users have orthogonal channels, is in the NQD region. This means that the use of NOMA for this case may result in a throughput loss compared to DPC, even though the use of NOMA can still offer other advantages, especially in overloaded scenarios in which the number of users exceeds the available resources. By using RISs and tuning the RIS phase shifting matrix, it is possible to reconfigure the users' channel vectors such that they satisfy the quasi-degradation criterion. For example, Fig. 6(b) reveals that by using an RIS with ten reflecting elements, the NQD region can be significantly reduced, compared to the case without an RIS shown in Fig. 6(a). In other words, if there are a sufficient number of reflecting elements on the RIS, it can be ensured that the use of RIS-NOMA yields the same performance as DPC, regardless of what the users' original channel conditions are. Furthermore, since both NOMA users occupy only a single spatial dimension, the remaining dimensions can be used to accommodate additional users.

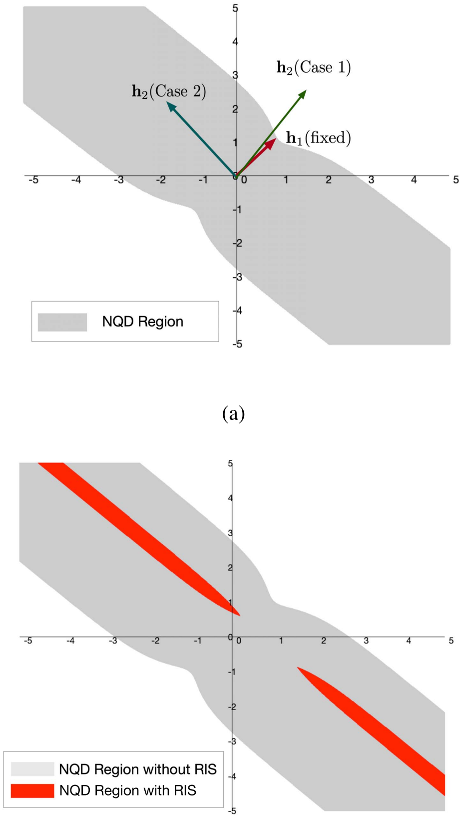

(a)

(b)

Fig. 6. ***Improvement of the quasi-degradation region by using RIS, with $h_1 = [1 \quad 1]^T$ and the two users' target data rates being 1 BPCU. G and g_i, $i \in \{1, 2\}$, are randomly generated. NQD represents nonquasi-degradation. (a) NQD without RISs. (b) RIS with ten reflecting elements.***

A more formal study of the impact of RISs on the quasi-degradation criterion was provided in [40], where a new expression of the quasi-degradation criterion for MISO-RIS-NOMA was developed. While the quasi-degradation criterion sheds light on whether NOMA can realize the same performance as DPC, it still has a few limitations. For example, the expressions for the quasi-degradation criterion reported in [40] have been developed by fixing the SIC decoding order, whereas recent studies have shown that opportunistically choosing the SIC decoding order can yield significant performance improvement in NOMA networks [41], [42]. Furthermore, the criterion has been investigated mainly for the simple two-user case, and its generalization to the more important overloaded cases, where the number of users exceeds the number of antennas at the BS, is still unknown.

C. Discussion and Outlook

As shown in Sections III-A and III-B, the integration of RISs and NOMA offers more flexibility for supporting

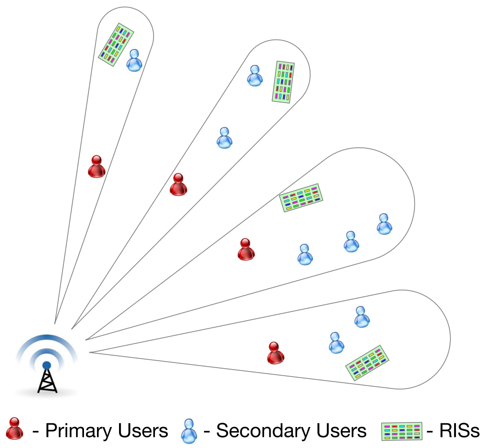

Fig. 7. ***Illustration of the benefit of RIS-NOMA, where primary users are served via conventional SDMA and the use of RIS-NOMA ensures that additional secondary users can also be served by an existing SDMA beam.***

massive connectivity and meeting the users' heterogeneous QoS requirements, compared to the two individual techniques alone. However, compared to SISO-RIS-NOMA and MISO-RIS-NOMA, the fundamentals of RIS-NOMA for more general setups, e.g., when there are multiple RISs and/or when each node is equipped with multiple antennas, have been less investigated in the literature, because of their challenging nature. A promising approach in this regard is to combine RIS-NOMA with conventional space-division multiple access (SDMA). Fig. 7 shows this approach, where conventional SDMA is used to form orthogonal beams and serve multiple primary users [36]. Assume that there are additional secondary users to be connected. Conventionally, it is not possible to serve these additional users directly with the existing spatial beams since the secondary users' channels may not be perfectly aligned with the primary users' channels due to the random radio propagation environment. The use of RISs opens the possibility of reconfiguring the propagation environment and aligning the secondary users' channel vectors with the existing SDMA beams [43]. As a result, the additional secondary users can be served without changing the SDMA legacy system, as shown in Fig. 7. In Section IV, more sophisticated RIS-NOMA designs for resource allocation will be discussed.

IV. DYNAMIC RESOURCE ALLOCATION FOR RIS-NOMA

Driven by the benefits of RIS-NOMA systems, such as their high spectral/EE, resource allocation/optimization has attracted significant research attention to further improve the communication performance. In particular, by jointly optimizing the communication resources, e.g., beamforming, power, and subchannels, and the reflecting coefficients of the RISs, the strength of the received signal can be significantly improved. In this section, we review traditional resource allocation methods, the related optimization problems, and their solutions in the context of RIS-NOMA systems, including throughput/data rate maximization, power minimization, and EE maximization, as summarized in Table 1. Subsequently, we discuss AI/ML-based resource allocation in RIS-NOMA.

A. Throughput/Data Rate Maximization

Due to the nonconvexity of the optimization problems formulated for throughput maximization, the alternating optimization (AO) algorithm proposed in [44] is widely adopted to design the transmit beamforming at the BSs and the RIS phase shifts in an alternating manner. Let us start with a simple system model, i.e., an SISO system. The average sum rate of a two-user downlink SISO-RIS-NOMA network was maximized by alternatively adjusting the phase shifts (using either dynamic phase adjustment or one-time phase adjustment) and the power allocation [45]. Considering a wireless-powered RIS-NOMA system with multiple devices/users, Wu *et al.* [46] first proved that dynamic phase shifts are not needed for downlink NOMA and uplink NOMA systems, which simplifies the problem and reduces the signaling overhead. In addition to the optimization of the beamforming at the BS and the phase shifts of the RIS, the channel assignment and decoding order of the NOMA users were optimized to maximize the system throughput [47]. To compare three multiple access techniques, namely, NOMA, frequency-division multiple access (FDMA), and time-division multiple access (TDMA), the weighted sum rate was studied for RIS systems in [48]. In this work, a joint optimization algorithm for the deployment location and the reflection coefficients of the RIS as well as the power allocation was proposed and shown to achieve near-optimal performance. Furthermore, the use of a BS equipped with multiple antennas was considered in RIS-NOMA systems [49], where a scheme for jointly optimizing active beamforming at the BS and the passive beamforming at the RIS was proposed in order to maximize the sum rate. Besides the downlink case, the sum-rate maximization problem was also studied for uplink RIS-NOMA systems [37].

RIS-NOMA is highly compatible with other key technologies for 6G communication systems, including millimeter-wave (mmWave) [50], [51] and massive MIMO [52]. Zuo *et al.* [50] considered the design of mmWave networks and proposed an optimization algorithm for maximizing the system sum rate, where the power allocation and reflection coefficients were optimized alternately. The results shown in [50] illustrate the effectiveness of integrating RISs in mmWave-NOMA systems. Recall that the small wavelength of mmWave signals enables the deployment of a large number of antennas, which motivates the design of mmWave massive MIMO systems. Liu *et al.* [51] considered the application of RIS-NOMA in mmWave massive MIMO systems, where the effects of the power leakage and the per-antenna power constraint were jointly investigated. In this work, two multibeam selection strategies were proposed to maximize the system weighted sum rate by jointly optimizing the active beamforming at the BS and the passive beamforming at the RIS. Regarding imperfect SIC in NOMA, the capabilities of RISs to manipulate wave polarization in dual-polarized MIMO-NOMA networks was investigated in [52], where the proposed novel strategy can alleviate the impact of imperfect SIC and exploit polarization diversity.

B. Power-/Energy-Efficient Resource Allocation

In future wireless communication networks, power efficiency and EE are important metrics for evaluating the network performance. For transmit power minimization, the performance of NOMA and OMA was compared in [34], which provides an important guideline for user pairing in RIS-aided systems with large numbers of users and resource blocks. Considering a single-cell RIS-NOMA network with multiple users, Fu *et al.* [55] proposed a novel difference-of-convex (DC) programming algorithm for the design of beamforming and phase shifts in order to minimize the total transmit power. To reduce the decoding complexity of NOMA transmission, users are generally grouped into small-size clusters in practice. Thus, a multicluster MISO RIS-NOMA system was studied in [56] aiming to minimize the total transmit power. In this work, a beamforming and phase shift optimization scheme based on second-order cone programming (SOCP) and alternating direction method of multipliers (ADMM) was proposed to minimize the total transmit power at the BS. Different from single-RIS-assisted NOMA networks [40], a multi-RIS and multicluster NOMA network was investigated in [57], where the joint optimization of the beamforming at the BS, the power allocation to the NOMA users, and the phase shifts of the RISs was proposed to minimize the transmit power at BS.

EE is another important metric for future green communication networks. EE is defined as the ratio between the amount of information bits delivered and the amount of energy consumed. In particular, different from sum-rate maximization and transmit power minimization, the aim of EE maximization is to achieve the optimal tradeoff between sum-rate maximization and power minimization, which leads to a fractional programming problem. Generally, the Dinkelbach algorithm can be used to iteratively achieve the system maximum EE by transforming the fractional form objective function into a subtractive-form one, which has been well investigated for NOMA systems [59]. Moreover, DC programming can also be utilized to maximize the EE of NOMA systems with matching theory-based subchannel allocation [60]. Driven by the benefits of RIS-NOMA, the EE maximization problem was first studied for two-user RIS-NOMA networks [58], where successive convex approximation (SCA)-based beamforming optimization and SDR-based phase shift optimization schemes were proposed for maximization of the EE. For complex RIS-NOMA networks, such as multicell systems, game theory and matching theory are efficient tools to address the user association, user clustering, and subchannel allocation problems with a lower complexity compared to an exhaustive search. This can be combined with convex optimization and ML techniques for efficient resource optimization in RIS-NOMA systems.

C. AI-/ML-Based Beamforming Optimization for RIS-NOMA

As one of the most promising technologies in 6G, AI includes advanced ML techniques, such as supervised learning, unsupervised learning, and reinforcement learning (RL), to smartly address the dynamic and uncertain environments in RIS-NOMA systems. ML techniques, especially RL, can be exploited for beamforming optimization, phase shift optimization, and power allocation in RIS-NOMA systems. To reduce the high computational complexity of the traditional resource allocation methods such as SDR and SCA, deep learning (DL) and RL can be utilized for optimization in RIS networks. In particular, DL can be used to optimize the RIS reflection matrix based on the sampled channel knowledge [61]. A deep neural network (DNN) was proposed for RIS configuration in an indoor RIS communication system [62]. In this work, the trained DNN is fed with the measured position information of the target user to determine the optimal phase configurations of the RIS.

Integrating NOMA into RIS can further improve the spectral efficiency and massive connectivity. However, as decoding complexity increases with the number of users, user grouping/clustering are widely adopted in NOMA systems, especially dynamic user grouping/clustering policies. Recently, intelligent user grouping/clustering methods, such as deep Q-network (DQN)-aided user clustering [63], have been proposed for NOMA systems to adapt to dynamic network conditions. Regarding the deployment design of MISO-RIS-NOMA networks, a decaying double DQN (D^3QN)-based algorithm was proposed to optimize the position and phase shifts of an RIS in [64]. In this work, the EE was maximized by the proposed D^3QN method, which is capable of overcoming the issue of large overestimation of action values raising in conventional Q-learning.

To support ultrafast communication in RIS-NOMA networks, the resource allocation, including the user grouping/clustering, subchannel assignment, beamforming design, power allocation, and phase shift optimization, must embrace intelligence to adapt to the fast time-varying wireless environment. Therefore, ML algorithms, such as DQN, have been utilized to provide smart control for RISs in NOMA networks [65]. In particular, in a MISO-RIS-NOMA system, a K-means-based method and a DQN-based algorithm were proposed [65] for user clustering and the joint design of the phase shift matrix and the power allocation, respectively. However, DQN can only handle discrete actions, such as quantized phase shifts. As a sophisticated deep RL method, deep deterministic policy

Table 1 Summary of Resource Allocation Schemes

Category	System Model (Reference)	Optimization Variables	Main Results
Throughput or Data Rate Maximization	SISO-RIS-NOMA [45]	Power & phase shift	Proposes two phase shift adjustments to maximize the average sum rate of two users
	SISO-RIS-NOMA [47]	Power & phase shift & channel allocation & decoding order	Proposes matching-based channel allocation and a joint optimization algorithm to maximize the system throughput
	SISO-RIS-NOMA [48]	Deployment location & reflection coefficients of RIS & power allocation	Compares NOMA, FDMA, and TDMA with respect to their weighted sum rates
	MISO-RIS-NOMA [49]	Active beamforming at BS & phase shifts of RISs	Proposes an efficient alternating algorithm to maximize the system sum rate by considering ideal RIS and non-ideal scenarios
	MISO-RIS-NOMA [37]	Active beamforming at BS & phase shifts of RISs	Provides a near-optimal solution to maximize the uplink sum rate
	mmWave aided RIS-NOMA [50]	Active beamforming at BS & phase shifts of RISs & power allocation	Confirms the effectiveness of introducing RISs in mmWave-NOMA systems
	mmWave aided massive MIMO RIS-NOMA [51]	Beam selection & active beamforming at BS & phase shifts of RISs	Confirms the weighted sum rate performance gain
	Massive MIMO RIS-NOMA [52]	Phase shifts of RISs	Confirms that dual-polarized RISs can facilitate cross-polar transmissions
	UAV-aided RIS-NOMA [53]	Placement and transmit power of UAV (RIS) & phase shifts of RIS	Provides a simple horizontal position design and beamforming design for a UAV and RIS phase shift optimization to maximize the strong user's data rate
	Multi-UAVs aided multiuser RIS-NOMA [54]	Placement and transmit power of UAVs & phase shifts of RISs & decoding order of NOMA users	Proposes a block coordinate descent (BCD)-based iterative algorithm to maximize the sum rate for a multi-UAV enabled NOMA-RIS network
Power Minimization	SISO-RIS-NOMA [34]	Active beamforming at BS & phase shifts of RISs	Provides a guideline for user pairing in RIS-NOMA systems with a large number of users and resource blocks
	MISO-RIS-NOMA [55]	Active beamforming at BS & phase shifts of RISs	Proposes an alternating DC method to minimize transmit power
	MISO-RIS-NOMA [56]	Active beamforming at BS & phase shifts of RISs	Proposes SOCP-ADMM based algorithm to achieve significant performance gains over conventional semidefinite programming (SDP) based algorithm
	MISO-RIS-NOMA [57]	Active beamforming at BS & phase shifts of RISs & power allocation coefficients	Proposes a joint optimization of the beamforming, the power allocation and the phase shifts of RISs for a multi-RIS aided NOMA system
	MISO-RIS-NOMA [40]	Active beamforming at BS & phase shifts of RISs	Provides a closed-form beamforming design to achieve the same performance as dirty paper coding
EE Maximization	MISO-RIS-NOMA [58]	Active beamforming at BS & phase shifts of RISs	Provides a simple beamforming and phase shift optimization scheme to maximize the system energy efficiency

gradient (DDPG) combines DQN and the policy gradient algorithm and is applicable to the DQN problem with continuous actions, such as continuous power allocation. DDPG is an effective actor–critic, model-free RL algorithm and is applicable to communication problems modeled based on the Markov decision process. There are three main elements in RL, i.e., the state space (wireless environment), action space (power allocation), and reward (sum rate). The agent (generally the BS) interacts with the dynamic wireless environment to generate good actions to maximize the long-term reward of the system, such as the sum rate. Thus, the phase shifts of RISs can be designed by DDPG in RIS-NOMA systems [66]–[68].

D. Discussion and Outlook

For resource optimization in RIS-NOMA systems, most formulated problems are nonconvex, such as the sum-rate maximization [37], [47], [48] and EE maximization [58] problems. Generally, nonconvex problems can be approximately transformed into convex ones by using SCA [58]. Then, convex optimization methods such as SDR [58] and DC programming [55] can be applied to achieve high performance with insightful closed-form solutions. However, the use of most convex optimization-based methods can result in high complexity, particularly in dynamic wireless environments, e.g., with rapidly time-varying channel conditions. For these dynamic wireless environments, ML/AI can be used to achieve efficient and low-complexity resource optimization. In the existing resource allocation works on RIS-NOMA systems, nonconvex/convex optimization methods and AI/ML have been separately applied in both fixed and dynamic wireless scenarios. The envisioned wireless networks of the future, e.g., the 6G network, will be more complex and more complicated than the current networks. Channel estimation, user association/grouping, power allocation, and beamforming design are vital challenges and closely intertwined. To design efficient resource allocation schemes ensuring high performance and low computational complexity, the synergistic combination of nonconvex/convex optimization methods and AI/ML will be needed. For example, for the multi-RIS-assisted NOMA system shown in Fig. 7, a closed-form solution can be derived by employing nonconvex/convex optimization methods in each user group [40]. Meanwhile, efficient AI-/ML-enabled resource allocation solutions with closed-form solutions as inputs can be designed for the entire network. Moreover, the model training needed for AI/ML methods consumes significant processing time and computing resources and is usually carried out offline. This introduces a huge transmission overhead and privacy issues in AI/ML-enabled RIS-NOMA systems. Federated learning (FL) is an attractive solution to shift the learning stage to the edge users for designing a communication-efficient scheme to achieve data privacy [69].

V. SECURITY PROVISIONING FOR RIS-NOMA

Due to the nature of the shared wireless medium, NOMA systems are prone to security attacks. Compared to conventional OMA systems, the use of NOMA leads to additional risks for information leakage [70]. For example, by multiplexing multiple signals at the transmitter side, an eavesdropper that receives the superimposed signal can potentially decode the messages of all users contained in the superimposed signal. Moreover, in NOMA transmission, users may act as eavesdroppers and take advantage of SIC to overhear the signals of the other users [71]. This motivates the application of an RIS to reconfigure the wireless propagation environment and provide energy-efficient jamming service against eavesdroppers. Furthermore, by intelligently exploiting the RIS phase shift uncertainty and the nonorthogonal signaling of NOMA, strong wireless communication covertness can be achieved [72]. The above considerations motivate a deeper investigation of physical layer security and covert communication in connection with RIS-NOMA.

A. Physical Layer Security With RIS-NOMA

In conventional NOMA networks, guaranteeing perfect security (i.e., achieving a positive secrecy rate) for all users is a challenging task [73]. Consider a multiuser NOMA scenario, where the quality of the channels from a transmitter to some of the legitimate users is worse than that of the wiretap channel from the transmitter to the eavesdropper. This situation can happen frequently in practical NOMA networks since users generally have different geographical locations and the eavesdropper may be closer to the transmitter. In this scenario, positive secrecy rates cannot be guaranteed if the transmitter and these users have one antenna only and cannot employ secure beamforming. This thus motivates the application of RISs to NOMA for physical layer security enhancement, the benefits of which are summarized next.

1) Improving Secrecy Rate: Theoretically, by deploying the RIS in the vicinity of the legitimate NOMA users or the eavesdropper and by properly designing the passive RIS beamforming, the signals received from the direct and reflected paths can add up constructively at the users but destructively at the eavesdropper [74]–[77]. Therefore, the legitimate signal reception quality is enhanced, while the eavesdropping capability is degraded, and an increased secrecy rate for RIS-NOMA can be achieved. Note that the design of the active beamforming at the transmitter and the passive beamforming at the RIS depends on the availability of channel state information (CSI). Compared to a scenario without secrecy considerations, enabling an efficient beamforming design to ensure communication security in RIS-NOMA systems requires additional CSI knowledge, i.e., the eavesdropper's CSI (ECSI) is required. However, the instantaneous ECSI is difficult to obtain in practice since the eavesdropper may intentionally remain silent and only its location information may be known corresponding to statistical ECSI, and although the local oscillator power leakage from the eavesdropper's radio frequency front end can be used for ECSI estimation, the acquired ECSI is expected to be outdated and imperfect. In [78], a robust secure beamforming strategy with artificial noise (AN) injection for RIS-NOMA was proposed by exploiting imperfect ECSI. The obtained results reveal that even with RIS, the use of AN is still helpful in degrading the eavesdropper's capability and improving the secrecy rate, particularly when the QoS requirements of the users are stringent. If only statistical CSI is available, it is not possible to maximize the secrecy rate directly. As an alternative, one can utilize the secrecy outage probability as the performance metric and impose an upper bound on it to limit the eavesdropping. In [79], a joint transmit and RIS beamforming scheme for distributed RIS deployment was proposed for RIS-NOMA, where the minimum nonadaptive secrecy rate (which is fixed and predetermined) among all users was maximized subject to a secrecy outage probability constraint. A significant secrecy rate improvement was observed compared to the scenario without RISs [79].

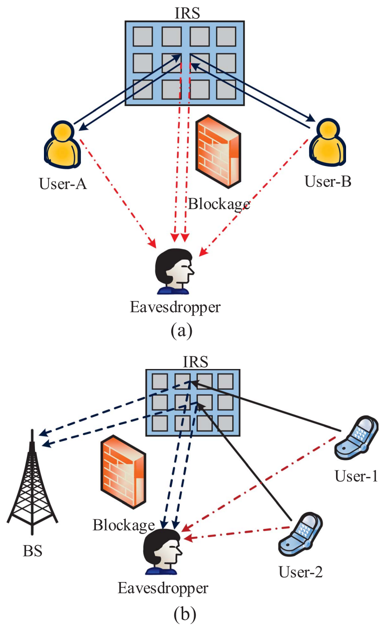

Fig. 8. ***Physical layer security with RIS-NOMA. (a) Signal overlapping. (b) Constellation overlapping.***

2) Creating Signal or Constellation Overlapping: In fact, the intentionally superimposed transmission of multiple signals via the RIS can result in desirable signal overlapping at the eavesdropper, and therefore, the eavesdropper has to adopt interference decoding and its signal reception quality is degraded. This can be demonstrated for a secure RIS-enabled two-way communication scenario, which can be regarded as a special case of NOMA [80]. As shown in Fig. 8(a), the two users simultaneously transmit their signals following the uplink NOMA principle and the RIS reflects the incident signals. On the one hand, each user can remove the interfering signal (a copy of which has been transmitted by the user itself) via self-interference cancellation without degrading its own signal reception quality. On the other hand, the eavesdropper receives a superimposed signal version and it has to decode one signal by treating the other signal as interference. Such an interfering signal can be used as a useful jamming signal to confuse the eavesdropper. Thus, by increasing the transmit power and/or the number of RIS's reflecting elements, the average secrecy rate can be improved [80]. Furthermore, the fundamental operating principle of RISs opens up a new design opportunity, i.e., causing the interuser interference in NOMA to be constructively and destructively received at the legitimate user and the eavesdropper, respectively. To clarify this, we consider the uplink NOMA scenario shown in Fig. 8(b). Two users transmit signals simultaneously to the BS via an RIS, where the RIS adjusts its phase to guarantee that the users' signal constellations fully overlap at the eavesdropper but do not overlap at the BS [71]. Thus, even if the eavesdropper may have a high received SNR to decode the superimposed signal successfully, the individual signals have to be recovered by random guess, which results in a poor bit error rate performance and degrades the eavesdropping capability significantly. To this end, a joint design of the power allocation and RIS beamforming is needed, which is an interesting direction for future research.

3) Generating Artificial Jamming Signals: Different from the conventional solutions that utilize RISs to reflect the confidential signal and the AN (which is generated by the transmitter) for physical layer security [81], [82], if appropriately modulated, the RIS can mimic a backscatter transmitter to generate artificial jamming when the signal is reflected to degrade the eavesdropper's reception. This approach is referred to as RIS-aided backscatter jamming [83]. By carefully optimizing the RIS's reflection coefficients, the information leakage to the eavesdropper can be minimized and reliable legitimate communication can be guaranteed. This strategy is particularly appealing due to the fact that the communication security is achieved without the consumption of additional resources to construct the AN, but by reusing the existing confidential signal and modulating it into a helpful jamming signal via the RIS to confuse the eavesdropper. Considering this merit, RIS-aided backscatter jamming is expected to be employed in NOMA networks for secrecy enhancement. However, in NOMA networks, interuser interference and backscatter jamming coexist, and both undoubtedly deteriorate the legitimate users' reception. Thus, extra efforts are required for interference management to balance communication reliability and security. One possible approach is to operate the RIS in a hybrid signal processing mode, i.e., partitioning the elements of the RIS into two groups: the elements in one group work in the reflection mode to improve the legitimate reception quality, while the elements in the other group work in the backscatter mode to generate the jamming signal for degradation of the eavesdropper. Based on this concept, future works may jointly optimize the elementwise mode selection and the corresponding modulation and reflection coefficients to maximize the overall system performance.

B. Covert Communication With RIS-NOMA

Under certain circumstances, safeguarding the content of communication by physical layer security techniques is not sufficient, and the communication entity may want to hide itself from being detected. This calls for covert wireless communication, which aims at hiding the amount of confidential data that are exchanged between a transmitter and a receiver, subject to a negligible detection probability of a warden. Several existing research works have shown that both NOMA and RISs can benefit communication covertness, since with NOMA, the transmission of a noncovert user can serve as a shield for a covert user [84] and the RIS enables signal strength boosting at the receiver and signal cancellation at the warden without consuming additional communication resources, thus guaranteeing green covertness [85].

However, solely using NOMA or RISs for covert communication has some disadvantages. In particular, other uncertainty sources, such as a random transmit power [84] or noise uncertainty at the warden [85], are required to achieve covertness. Assume that a transmitter communicates with a receiver by applying RIS-assisted OMA or NOMA without RIS. Covertness cannot be achieved in either scenario since, in both cases, the warden can exactly measure its nonzero received power to detect the covert transmission. This thus motivates the integration of NOMA and RISs toward covert communication, where the NOMA signaling of a noncovert user and the phase shift uncertainty of the RIS are jointly exploited as the new cover medium to hide the covert user's transmission [72], [86]. As validated in [72] and [86], by appropriately generating a random phase shift pattern at the RIS, uncertainties exist in the warden's received signal power. In fact, the detection error probability of the warden increases with the transmit power and the number of RIS elements.

C. Discussion and Outlook

As shown in Sections V-A and V-B, the use of RISs in NOMA systems can significantly enhance the secrecy and covert communication performance. Apart from the above progress, there are several interesting yet unsolved issues. For example, many existing works on physical layer security assume that the eavesdropper operates in a passive mode for information interception. However, in practical wireless NOMA networks, the eavesdropper may dynamically change the mode of attack based on its channel condition, e.g., the eavesdropper may perform passive eavesdropping if it has a strong eavesdropping channel; otherwise, it may employ jamming to disrupt the legitimate signal reception [71]. Moreover, the eavesdropper may be equipped with full-duplex transceivers and perform simultaneous eavesdropping and jamming [87]. How to exploit an RIS to combat an adaptive and/or full-duplex eavesdropper in NOMA systems requires additional research. For covert communication with RIS-NOMA, it is assumed that the number of channel uses is infinite and the RIS phase shifts are continuous [72], [86], which may not always be feasible in practice. For future work, it is important to investigate the robust design of RIS-NOMA systems to enable covert communication with consideration of a finite number of channel uses and discrete phase shifts.

VI. PRACTICAL IMPLEMENTATION OF RIS-NOMA

In this section, three practical implementation issues for RIS-NOMA, namely, channel estimation, robust design, and deployment, are discussed in detail.

A. Channel Estimation

To fully reap the various performance gains brought by RIS-NOMA, efficient channel estimation schemes are required since both active transmit beamforming at the BS and passive reflection beamforming at the RIS rely on CSI. However, this is a nontrivial task since the RIS does not have any RF chains to enable pilot signal transmission for channel estimation and there is a large number of RIS-related channel coefficients, due to the large number of RIS elements and the multiuser nature of NOMA, which need to be estimated. In the literature, two kinds of RIS channel estimation schemes have been developed for the case when the RIS is integrated with sensing devices and when this is not the case [88], as elaborated in the following.

1) Semipassive RIS Channel Estimation: In this scheme, additional sensing devices (e.g., low-cost sensors) are integrated into the reflecting elements of the RIS. Hence, by letting the BS and each user transmit pilot signals, the channels from the BS/users to the RIS can be estimated based on their received pilots, and the corresponding reverse channels can be easily obtained by exploiting channel reciprocity in a time division duplex (TDD) system. To reduce the cost and energy consumption of semipassive RIS, the number of integrated sensors is usually less than that of the reflecting elements. This indicates that the estimated channels are only a subset of all channels, and the available estimated channels are to be used to recover the high-dimensional full channels. In fact, sparsity or spatial correlations between the estimated and the actual channels may exist. To this end, advanced signal processing techniques, e.g., compressed sensing and ML, can be applied for channel estimation. In [62] and [91], compressed sensing and DL-based semipassive RIS channel estimation schemes were proposed, where the channel sparsity and the mapping information of the sampled channels were exploited to construct the full channels. The results show that the proposed schemes achieve a comparable rate performance as the case with perfect channel knowledge while employing a negligible training overhead and a small number of active sensors. By assuming sparse channels in the beamspace domain, Alexandropoulos and Vlachos [90] developed an efficient AO method to explicitly estimate the channels of the RIS elements attached to a single RF chain, where the impact of the channel sensing time on the mean-squared error (MSE) performance was analytically evaluated. Note that the above solution approaches are only applicable in TDD systems, while the design of semipassive RIS channel estimation schemes in frequency-division duplex systems is still an open issue.

2) Fully Passive RIS Channel Estimation: If the RIS is fully passive and does not possess any active sensors, it is not possible to estimate the CSI between the BS/users and the RIS directly. As an alternative approach, one can estimate the cascaded BS-RIS-user channels instead. Basically, the cascaded channel knowledge can be estimated following an ON/OFF RIS reflection pattern-based scheme [91], where for each training signal transmission, only one RIS reflection element is turned on, while the others are turned off, and this process is carried out until all the RIS reflecting elements have been turned on. As a result, the cascaded BS-RIS-user CSI for each reflecting element is obtained in a sequential manner. We note that this scheme inevitably incurs a very large training overhead for pilot signal transmission, i.e., N pilot symbols are needed if the RIS is equipped with N reflecting elements. To overcome this issue, an RIS reflecting element grouping-aided channel estimation scheme was proposed in [94] and [95], where adjacent RIS reflecting elements were grouped into a subsurface, as channels associated with the same subsurface are usually spatially correlated. As such, only the cascaded channels for each subgroup have to be estimated, which largely reduces the training overhead. The above fully passive channel estimation schemes consider only a single user and need to be suitably modified to fit multiuser NOMA networks. Intuitively, one can estimate the cascaded channels for K users by sequentially using the single-user schemes K times, which, however, significantly increases the training overhead, especially when K is large. A potential approach is to treat the K users as one equivalent K-antenna user and exploit certain RIS channel properties (e.g., low rank, spatial correlation, and sparsity) to facilitate the decomposition of the cascaded channel matrix for channel estimation [94]–[96]. Another promising approach is to exploit the fact that all the users share the same BS-RIS channel, and hence, one user can be selected as the reference user and his/her cascaded channel is estimated first. Subsequently, the remaining $K-1$ users' cascaded channels can be obtained by individually scaling the reference user's cascaded channel [88]. The optimal user selection criterion and a mechanism to learn the relationship between the users' cascaded channels should be further investigated.

We note that, compared with OMA, accurate CSI knowledge is more important in NOMA systems due to the use of the SIC receivers. This thus puts forward higher demands for RIS-NOMA channel estimation. For RIS-OMA channel estimation, the training signals are designed with pairwise orthogonality to guarantee CSI estimation accuracy. However, in the context of RIS-NOMA with a massive number of users, the design of accurate channel estimation is more challenging since the number of possible orthogonal sequences may be smaller than the number of users. One effective solution is to increase the length of the training sequences and, hence, the number of orthogonal sequences, which, unfortunately, reduces the spectral efficiency. Alternatively, nonorthogonal training sequences can be used as an alternative for channel estimation in massive RIS-NOMA networks. However, the use of nonorthogonal training sequences can lead to nonnegligible channel estimation errors. The robust design of RIS-NOMA networks in the presence of imperfect CSI will be discussed in Section VI-B.

B. Robust Design

Despite the above progress in channel estimation for RIS-aided systems, channel estimation errors are inevitable in practice due to the limited training resources (such as power and time), the imperfections of the RIS hardware, and the CSI feedback latency, resulting in performance degradation. Thus, designing robust transmission schemes to reduce the performance degradation of RIS-NOMA is a critical but also a challenging task. On the one hand, existing works [97]–[99] proposed robust beamforming designs for imperfect cascaded BS-RIS-user channel knowledge at the BS for OMA, but these results cannot be applied to NOMA directly. This is because with NOMA, the SIC decoding order depends on the users' estimated channel gains, which causes the SIC decoding order and the active/passive beamformers to be highly coupled. To resolve this problem, an intuitive method is to first fix the SIC decoding order and design the robust active/passive beamformers using the imperfect cascaded BS-RIS-users' channel knowledge and then adopt an exhaustive search to find the optimal decoding order for the obtained beamformers [49]. However, the complexity of this scheme is high, especially when the number of NOMA users is very large. An alternative approach is to simply use the imperfect direct BS-users' channel information for SIC decoding order design, but this may lead to poor performance since the effect of the imperfect cascaded BS-RIS-users' channel information is not considered. Thus, novel robust RIS-NOMA designs with imperfect CSI are needed for a balanced tradeoff between performance and complexity. On the other hand, at the NOMA receivers, the channel estimation errors cause additional interference at each SIC stage such that the signals in the later SIC stages may suffer from severe interference, which leads to a high probability of decoding errors. Therefore, the transmission rates and active/passive beamformers should be carefully designed to account for the imperfect CSI for reliable NOMA transmission [100]. Furthermore, as indicated in [101], when CSI errors become a severe issue, controlling the RIS reflection amplitudes can be a low-cost alternative to the conventional reflection phase beamforming, yet offering comparable and even more favorable performance.

Estimation of the instantaneous CSI in RIS-NOMA networks inevitably consumes a significant number of time slots, proportional to the number of RIS reflecting elements and the connected NOMA users. The resulting overhead becomes excessive when the numbers of reflecting elements and NOMA users are large. Due to the limited duration of the channel coherence time, less time is left for payload NOMA transmission. Hence, it may be more practical to design the RIS phase shifts based on statistical CSI, which varies much more slowly than the instantaneous CSI. By utilizing the ergodic sum rates of all users as performance metric, the joint active and passive beamforming can be designed based on the average channel gains [11], [102]–[107]. Furthermore, to compensate for the performance loss caused by solely using the statistical CSI, a two-timescale beamforming scheme can be applied, where the long-term RIS phase shifts are designed based on the statistical CSI of all links, and the short-term active beamforming at the BS is designed to cater to the instantaneous CSI of all users' reconfigured channels with optimized RIS phase shifts [108]–[110]. As a result, performance gains in terms of an improved achievable data rate can be achieved. When applying the above two-timescale beamforming in RIS-NOMA networks, additional constraints imposed by the SIC decoding order need to be satisfied, which requires efficient algorithms for the joint optimal SIC decoding order and beamforming design.

In practical RIS-NOMA systems, hardware impairments at the transceivers are inevitable. For example, practical RISs employ discrete phase shifts and/or discrete reflection amplitudes for cost and energy saving, which degrades the communication performance compared to the ideal case without hardware impairments. In addition, for NOMA, the design of SIC is not a trivial task, especially if the number of connected users is extremely large. Different users may have different signal detection capabilities and CSI availabilities, and users with low detection capability and/or inaccurate CSI will suffer from decoding errors in SIC, i.e., imperfect SIC [111]. Even worse, the decoding

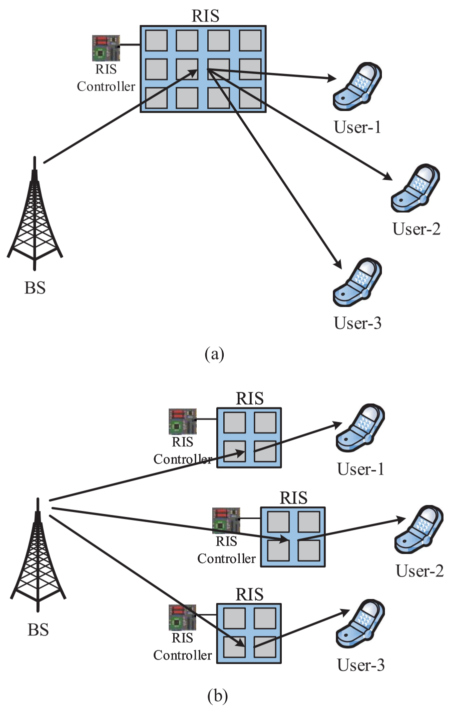

Fig. 9. ***RIS deployment strategies. (a) Centralized. (b) Distributed.***

errors in the preceding SIC stages may affect the interference cancellation in the current stage, giving rise to error propagation effects. The design and analysis of RIS-NOMA with hardware imperfections have not been comprehensively considered in the literature, which motivates future research in this direction.

C. Deployment Strategy

From an implementation perspective, the RIS deployment plays an important role in boosting the performance of NOMA networks. Given a fixed number of the reflecting elements, the RIS can be either deployed in a centralized manner with all the reflecting elements forming a large RIS located close to the BS/user side or in a distributed manner where the reflecting elements form multiple RISs and each RIS is located near one of the users [88], as shown in Fig. 9. Thus far, there is no consensus on whether the centralized RIS deployment or the distributed RIS deployment is more preferable for NOMA networks, and in fact, both deployment strategies have their own benefits and drawbacks.

1) *Centralized RIS deployment:* This strategy is appealing for the cluster-based NOMA scenario where the direct communication links from the BS to the users are highly correlated (e.g., in mmWave and terahertz (THz) communications) [112]. In this scenario, the BS may not have enough DoFs to enable user clustering via the transmit beamforming. This motivates the use of a centralized RIS to provide additional DoFs. Theoretically, a centralized RIS has a large number of reflecting elements to facilitate beamforming, and a high passive array gain is obtained for user clustering [112]. As indicated in [113], the gain of NOMA over OMA is more pronounced when the users have distinct channel conditions. The centralized RIS deployment can help achieve this. By deploying the RIS in an asymmetric manner to enlarge the disparities among the users' channels, a larger sum rate is achieved with NOMA compared to OMA [48]. Furthermore, for a special two-user NOMA scenario under the twin channel condition (i.e., the BS-RIS-user channels are similar to each other), it was shown in [114] that the centralized RIS deployment always offers a larger multiuser achievable rate region than the distributed RIS deployment. However, considering the size and hardware constraints, it is not always feasible to deploy a huge centralized RIS, while deploying multiple moderate- or small-size RISs at their respective user clusters is more manageable [88].
2) *Distributed RIS deployment:* This strategy is ideal for the scenario where the locations of the users are clustered. The advantage of applying distributed RISs in this scenario lies in the fact that different NOMA user clusters are associated with different RISs and are separated by large distances, and thus, the signals reflected by one RIS have little impact on the reception performance of other unintended user clusters [112]. Moreover, with proper placement, the distributed RIS deployment will very likely create more line-of-sight (LoS) paths between the BS and the users compared to the centralized RIS deployment when users are randomly located [36]. Despite the above merits, the distributed RIS deployment suffers from a high signaling overhead since the RIS phase shift design requires information exchange between the BS and multiple RIS controllers.

To be specific, relying on centralized or distributed RIS deployment alone may not satisfy all the requirements of NOMA transmission, and a more general hybrid RIS deployment may be desirable [115]. In the hybrid design, a large centralized RIS is deployed close to the BS to provide a high passive beamforming gain, while multiple small RISs are deployed close to the users to support multiple LoS channels. Hence, the hybrid RIS deployment combines the complementary advantages of the centralized and distributed strategies and can achieve a tradeoff between them. A joint optimization framework for transmit beamforming, all RISs' reflection beamforming, and RIS element allocation (i.e., for a fixed number of RIS elements, the number of elements assigned to the centralized RIS and each distributed RIS) is required to improve the overall system performance. This requires further investigation in the future.

D. Discussion and Outlook

In this section, we have highlighted several practical implementation issues for RIS-NOMA networks, including channel estimation, robust design, and deployment strategy. These practical issues are inevitable in any RIS-NOMA design and application. This paves the way for a multitude of a new research problem concerning efficient and robust RIS-NOMA designs in future wireless networks. However, there are still some challenges that have not been addressed yet. For example, most existing works on RIS-NOMA channel estimation considered the TDD setting. Although TDD facilitates RIS channel estimation if channel reciprocity holds, this may not always be the case. One recent work showed that the RIS phase shifts depend on the incident angles of the electromagnetic waves, and in this case, channel reciprocity does not hold [116]. Therefore, it is imperative to study novel channel estimation and feedback designs for RIS-NOMA networks, which is challenging due to the large dimensional channel matrices (e.g., due to a large number of RIS reflecting elements and NOMA users). Furthermore, for distributed RIS deployment in NOMA systems with randomly distributed users, it is likely that all users are located close to one of the RISs, which is necessary to achieve optimal performance [79]. In this situation, the distances from a RIS to the different users associated with it may not be equal. This implies that some of the users may be in the near field of the distributed RISs and the far-field channel model does not hold. To this end, it is important to develop new physics-based models for practical RIS-NOMA systems and investigate thr corresponding efficient approximation methods to obtain tractable channel statistics to facilitate performance evaluation.

VII. FUTURE DIRECTIONS AND EMERGING APPLICATIONS OF RIS-NOMA

In this section, we explore the potential of employing RIS-NOMA in various emerging wireless network architectures.

A. RIS-NOMA-Assisted Aerial Radio Access Networks

Aerial radio access networks are a promising strategy to complement the conventional terrestrial cellular communications [117]. Comprising airborne components such as UAVs, aerial radio access networks can quickly establish a flexible access infrastructure and support the development of seamless 6G mobile communication systems, where the use of RISs and NOMA can be particularly important, as discussed in detail in the following.

Being equipped with communication and signal processing capabilities, UAVs can act as moving BSs or relays to facilitate reliable and efficient communication with multiple users [118], [119]. Ideally, UAVs with high mobility can adapt their positions dynamically according to the changes in the communication environment and thus can maintain virtual LoS links between transceivers. However, when the users are roaming continuously, it is challenging for the UAV to periodically reposition itself according to the mobility of the users (as this could consume significant amounts of energy) since the UAV is usually powered by batteries without constant energy supply. RISs can be exploited to tackle this challenge. Specifically, one can adjust the phase shifts of the RIS instead of controlling the movement of the UAV to help establish reliable communication links between the UAV and the users. Moreover, with additional array gains provided by the RIS, only a small number of onboard antennas (which reduces the energy consumption of the UAV) are needed for the UAV to support the required array gains at the users [120]–[122]. On the other hand, by mounting RISs on UAVs to enable over-the-air intelligent reflection, 360° panoramic/full-angle reflection can be realized, i.e., aerial RISs can help reflect signals between any pair of nodes on the ground, which is in sharp contrast to conventional terrestrial RISs that can only serve users in a half-space [123]. To support massive connectivity in UAV networks, NOMA can be employed to encourage spectrum sharing among users over the same time/frequency resource block [124]. Nevertheless, RIS-NOMA-assisted UAV communications introduce new challenges. First, for the general scenario with multiple UAVs and/or RISs, the achievable rate of each user depends not only on the desired signal power level but also on the interference level. Thus, it is important to jointly design the 3-D UAV trajectory/placement, RISs reflection beamforming, and user association to maximize the achievable rate of the users. In addition, to fully reap the NOMA gains, additional channel condition/QoS-based decoding order design needs to be considered. This makes the joint UAV trajectory/placement, RISs reflection beamforming, and NOMA decoding order selection problem highly coupled and difficult to resolve. Compared to the fixed RIS deployment, e.g., on a building, deploying an RIS on a UAV can lead to a more significant improvement of the channel conditions by adjusting the UAV's mobility and/or the RIS reflection coefficients. In [53], a simple design of a UAV-aided RIS-NOMA system was proposed to maximize the strong user's data rate based on the UAV's optimized horizontal position. Different from [53], RISs can also be integrated into UAV-enabled communication systems to enhance the channel quality. Mu *et al.* [54] considered a more practical scenario, i.e., a multi-UAV and multiuser RIS-NOMA system [54]. In this work, the placement and transmit power of UAVs, the reflection matrix of the RIS, and the NOMA decoding order of the users were jointly optimized to maximize the sum rate of the entire system.

We note that the high mobility of UAVs generally results in more frequent handovers and time-varying wireless channels between UAVs and ground users, which, however, leads to critical challenges for off-line optimization. Furthermore, the UAVs' high mobility makes efficient channel tracking for ground users a more challenging task and may incur excessive pilot overhead. Therefore, it is necessary to develop new techniques and designs, e.g., efficient handover, resource management, and channel acquisition strategies, to tackle the issues caused by the high mobility of UAVs and guarantee seamless service provisioning for RIS-NOMA. Fortunately, AI/ML can be used to provide real-time control for UAV-enabled RIS-NOMA networks. By smartly controlling the UAV movement and adjusting the phase shifts of the RISs via ML techniques, the energy consumption of UAV-enabled RIS-NOMA networks can be minimized [125]. Recently, a novel RIS framework, namely, transmitting and reflecting RISs (STAR-RISs), was proposed, where signals are reflected and transmitted simultaneously, which can be seamlessly combined with the NOMA technology to achieve a high sum rate [126]. Similar to RIS-NOMA, STAR-RIS-NOMA can be implemented to provide reliable communication links between UAVs and users. By using ML techniques, both transmitting and reflecting phase shifts of STAR-RIS can be smartly controlled to improve the communication quality for UAV-enabled NOMA networks in terms of low energy cost, low latency, and high spectral efficiency.

Furthermore, there is increasing enthusiasm regarding high-altitude platforms (HAPs) and low Earth orbit (LEO) satellites for providing access services in remote areas, which do not have full terrestrial BS coverage, both from industry to academia. For example, SpaceX Corp is currently implementing the Starlink project, which establishes a constellation of thousands of small LEO satellites to support global network services [127]. Several companies are devoted to the research and development of HAPs, including the Zephyr Platform of Airbus [128], Stratobus Platform of Thales [129], and Solar HAPS of HAPSMobile [130]. The application of RIS in HAPs and LEO satellites can yield significant capacity and coverage enhancement. For example, by mounting RISs on HAPs and LEO satellites, the amount of energy consumed by the communication payload can be reduced, and the average flight duration of HAPs and LEO satellites can be increased [131]. Another example is the IoT networks, where by installing the RIS on LEO satellites, it is possible for ground-based IoT devices to track the velocities of the LEO satellites with high accuracy and low computational cost [132]. In addition, the use of NOMA can benefit both HAPs and LEO satellites in enabling massive connectivity between LEO satellites and HAPs, as well as between HAPs and terrestrial devices. Therefore, the communication performance can be further enhanced, e.g., in terms of spectrum efficiency, energy consumption, and network coverage. However, studies of RIS-NOMA-assisted HAP and LEO satellite communications are still in a nascent stage and advanced design and resource allocation algorithms have to be developed.

B. RIS-NOMA-Assisted MEC

MEC allows computation offloading to local servers for reducing the energy consumption and processing delay [133], [134]. The computation offloading performance gains can be further improved if NOMA and RISs are properly applied, as explained in the following.

1) From the delay perspective, the use of NOMA allows multiple users to complete their offloading at the same time or one user to offload multiple tasks to multiple MEC servers simultaneously, thus effectively reducing the offloading latency [135], [136]. In addition, from the energy perspective, by asking the strong user to first offload a portion of its task when the weak user is offloading with NOMA and then allowing the strong user to offload its remaining task using a dedicated time slot, the energy consumption for offloading can be significantly reduced [135], [137]. Moreover, the energy consumption of MEC networks can be substantially decreased by exploiting NOMA uplink transmission [138] and NOMA downlink transmission [100].
2) When the communication links for data and computation offloading are strongly attenuated, the use of RISs reflection beamforming can improve the channel quality to offload the computation tasks without incurring additional energy consumption, which facilitates low latency and high EE [139]–[141]. Furthermore, by utilizing the RISs to dynamically reconfigure the communication links for computation offloading, the offloading decisions and policies can be flexibly determined, thereby improving computation resource usage [88].

Hence, applying RIS-NOMA to MEC can facilitate more intelligent offloading management, by combining the benefits of RISs and NOMA in a constructive manner to further enhance the system performance. In [142], a new flexible time-sharing RIS-NOMA scheme for computation offloading was proposed, which allows users to flexibly divide their offloading data into two parts transmitted via RIS-NOMA and RIS-OMA. The results show that RIS-OMA outperforms RIS-NOMA in terms of sum delay minimization when the users' cloud-computing time is sufficiently long and/or the rate improvement of RIS-OMA over RIS-NOMA is sufficiently large. In [143], the joint optimization of the RIS reflection beamforming, power control, transmission rate and time, and NOMA decoding order for RIS-NOMA-assisted MEC was presented to minimize the total energy consumption. It was shown that compared to conventional RIS-OMA-assisted MEC, the proposed solution can dramatically decrease the total energy consumption of the system. Note that for a large-size MEC network with a massive number of users, edge servers, and RISs, it is still not known how to efficiently associate the users, the edge servers, and the RISs and how to optimally design the power allocation and RISs reflection beamforming. Therefore, these issues merit further investigation.

C. RIS-NOMA-Assisted WPT

WPT has been applied in the IoT networks for prolonging the battery lives of the devices and resolving the energy limitation problem [144], [145]. On the one hand, in recent years, the application of RISs to improve the efficiency of WPT to energy receivers has been studied. As indicated in [149] and [150], by properly designing the RIS reflection beamforming and deploying RISs to create LoS paths between the power beacon and the energy receivers, the received power of self-sustainable devices in the downlink can be enhanced, and this in turn increases the throughput performance of the uplink transmission due to the large available transmit power. Moreover, with joint transmit beamforming and RIS reflection beamforming, an improved rate–energy tradeoff can be achieved in WPT networks [148]–[150].

On the other hand, NOMA is also appealing in WPT networks since it enables the simultaneous access of massive numbers of users to improve the throughput, fairness, and EE [151], [152]. More recently, RISs have been integrated with NOMA and WPT for further performance improvement. In [46], RIS-NOMA-assisted WPT is investigated, where multiple devices first harvest energy from a hybrid access point and then transmit information using NOMA to the hybrid access point. An optimization framework for the RIS phase shifts and the resource allocation is developed to maximize the sum throughput of all the devices. Interestingly, it is found that downlink WPT and uplink information transmission share the same RIS phase shifts, and the proposed design can realize spectrum and energy-efficient wireless-powered communication networks. In [153], a hybrid NOMA and OMA scheme for RIS-assisted WPT networks was proposed to balance complexity and performance. In particular, the users are grouped into multiple clusters, where the users in the same cluster transmit information using NOMA, while the users in different clusters transmit information via OMA. Efficient user grouping and resource allocation algorithms were presented, which guarantee a sufficiently large network throughput. In [154], a BS power minimization problem for RIS-NOMA-assisted WPT networks was studied, and an efficient two-stage algorithm was proposed to jointly optimize the NOMA decoding order, BS transmit beamforming, power splitting ratio, and RIS reflection beamforming. It is shown that compared with non-RIS-assisted networks, the proposed design can reduce the BS transmit power by 51.13%. Despite the existing works discussed above, there are still several challenges, such as the impact of discrete RIS phase shifts, imperfect CSI and/or SIC, and nonlinear energy harvesting, which have not been thoroughly investigated for RIS-NOMA networks yet and require further research.

D. Exploiting New Spectral Resources via RIS-NOMA

One paradigm shift for the design of the next generation of mobile networks is the use of new spectrum, such as the mmWave, THz, and visible light frequency bands, because the frequency range below 6 GHz is almost fully allocated and occupied [1], [2]. The main advantage of using these new spectra is that there will be a huge amount of bandwidth available for wireless communications. For example, the use of the THz band between 0.1 and 10 THz is envisioned to be crucial for supporting emerging wireless services requiring multiple Tbps data rates, including autonomous driving and immersive VR/AR gaming [155].

The use of this new spectrum also poses new challenges for the design of next-generation mobile networks, which can be addressed by employing RIS-NOMA. For example, both visible light communications (VLCs) and THz communications are highly vulnerable to blockages due to their short wavelengths, which means that a direct communication link between the transmitter and the receiver can be easily broken [156], [157]. The fact that the THz waves suffer from additional propagation loss due to molecular absorption makes it even more challenging to establish a direct communication link between the transmitter and the receiver. The use of an RIS can provide a robust and spectrally efficient way to combat these detrimental propagation features of the THz and VLC bands, as an RIS can be used to connect the transmitter and the receiver if their direct link is weak or even broken.

Hardware impairments are another key challenge induced by the use of these new spectra. Take again THz communications as an example. The transmitters and receivers of THz networks are expected to be equipped with directional antenna arrays and high-performance gains are achievable only if the beams generated by these directional arrays are perfectly aligned [158]. However, in practice, THz networks are prone to misalignment errors, which results in a significant reduction in the received signal strength and, hence, in the spectral efficiency. Misalignment has also been recognized as a severe issue in free-space optical (FSO) communications, due to tracking errors of the FSO transceivers and building sway [159]. Fortunately, misalignment errors can be exploited by NOMA for improving spectral efficiency and user connectivity. For example, let us assume the beam generated by a THz BS is imperfect for its intended user. Without changing the beam, the use of NOMA can ensure that additional users can be served, as explained in the following. In future wireless networks, such as ultra-dense networks (UDNs) and massive IoT, it is very likely that there are many users whose channels are perfectly aligned with the existing beam. Therefore, by serving these additional users as the strong users via power-domain NOMA, the overall system throughput and user connectivity can be improved without consuming extra bandwidth [160].

While it is promising to apply RIS-NOMA in networks using these new spectra, there are still many open research problems. For example, for networks using THz frequencies or FSO links, an important direction for future research is to develop accurate yet insightful channel models, which are critical for identifying the fundamental limits of RIS-NOMA. In addition, the use of RIS-NOMA in THz networks requires fast scheduling to ensure that additional users can be opportunistically selected and served.

However, performing channel estimation in a timely and spectrally efficient manner is challenging.

VIII. CONCLUSION

In this survey, we have provided a comprehensive overview of recent progress on the efficient integration of RISs and NOMA. In particular, the basics of the two techniques were reviewed first, and then, the fundamentals of integrating RISs and NOMA were discussed for both SISO and MISO communication scenarios. Because resource allocation is crucial to the success of RIS-NOMA networks, various approaches for resource allocation design, including AI-empowered designs, were described. Security provisioning and practical RIS-NOMA implementation issues were also studied. Finally, the survey was concluded by a detailed discussion of promising future research directions and potential applications of RIS-NOMA. ■

REFERENCES

[1] X.-H. You *et al.*, "Towards 6G wireless communication networks: Vision, enabling technologies, and new paradigm shifts," *Sci. China Inf. Sci.*, vol. 64, no. 1, pp. 1–74, Jan. 2021.

[2] Z. Zhang *et al.*, "6G wireless networks: Vision, requirements, architecture, and key technologies," *IEEE Veh. Technol. Mag.*, vol. 14, no. 3, pp. 28–41, Sep. 2019.

[3] Y. Xiao, G. Shi, Y. Li, W. Saad, and H. V. Poor, "Toward self-learning edge intelligence in 6G," *IEEE Commun. Mag.*, vol. 58, no. 12, pp. 34–40, Dec. 2020.

[4] W. Saad, M. Bennis, and M. Chen, "A vision of 6G wireless systems: Applications, trends, technologies, and open research problems," *IEEE Netw.*, vol. 34, no. 3, pp. 134–142, Oct. 2020.

[5] M. D. Renzo *et al.*, "Smart radio environments empowered by reconfigurable AI meta-surfaces: An idea whose time has come," *EURASIP J. Wireless Commun. Netw.*, vol. 2019, no. 1, pp. 1–20, May 2019.

[6] Q. Wu and R. Zhang, "Intelligent reflecting surface enhanced wireless network via joint active and passive beamforming," *IEEE Trans. Wireless Commun.*, vol. 18, no. 11, pp. 5394–5409, Nov. 2019.

[7] Q. Q. Wu and R. Zhang, "Beamforming optimization for wireless network aided by intelligent reflecting surface with discrete phase shifts," *IEEE Trans. Commun.*, vol. 68, no. 3, pp. 1838–1851, Dec./May 2020.

[8] C. Huang, A. Zappone, G. C. Alexandropoulos, M. Debbah, and C. Yuen, "Reconfigurable intelligent surfaces for energy efficiency in wireless communication," *IEEE Trans. Wireless Commun.*, vol. 18, no. 8, pp. 4157–4170, Aug. 2019.

[9] E. Basar, M. Di Renzo, J. De Rosny, M. Debbah, M. Alouini, and R. Zhang, "Wireless communications through reconfigurable intelligent surfaces," *IEEE Access*, vol. 7, pp. 116753–116773, 2019.

[10] Q. Wu and R. Zhang, "Towards smart and reconfigurable environment: Intelligent reflecting surface aided wireless network," *IEEE Commun. Mag.*, vol. 58, no. 1, pp. 106–112, Nov. 2020.

[11] Y. Han, W. Tang, S. Jin, C. Wen, and X. Ma, "Large intelligent surface-assisted wireless communication exploiting statistical CSI," *IEEE Trans. Veh. Technol.*, vol. 68, no. 8, pp. 8238–8242, Jun. 2019.

[12] I. Al-Nahhal, O. A. Dobre, and E. Basar, "Reconfigurable intelligent surface-assisted uplink sparse code multiple access," *IEEE Commun. Lett.*, vol. 25, no. 6, pp. 2058–2062, Jun. 2021.

[13] C. Wu, Y. Liu, X. Mu, X. Gu, and O. A. Dobre, "Coverage characterization of STAR-RIS networks: NOMA and OMA," *IEEE Commun. Lett.*, vol. 25, no. 9, pp. 3036–3040, Sep. 2021.

[14] C. Pan *et al.*, "Reconfigurable intelligent surfaces for 6G systems: Principles, applications, and research directions," *IEEE Commun. Mag.*, vol. 59, no. 6, pp. 14–20, Jun. 2021.

[15] M. Vaezi, Z. Ding, and H. V. Poor, *Multiple Access Techniques for 5G Wireless Networks and Beyond*. Cham, Switzerland: Springer, 2019.

[16] Z. Ding, X. Lei, G. K. Karagiannidis, R. Schober, J. Yuan, and V. Bhargava, "A survey on non-orthogonal multiple access for 5G networks: Research challenges and future trends," *IEEE J. Sel. Areas Commun.*, vol. 35, no. 10, pp. 2181–2195, Oct. 2017.

[17] Y. Liu, Z. Qin, M. Elkashlan, Z. Ding, A. Nallanathan, and L. Hanzo, "Nonorthogonal multiple access for 5G and beyond," *Proc. IEEE*, vol. 105, no. 12, pp. 2347–2381, Dec. 2017.

[18] Z. Ding *et al.*, "Application of non-orthogonal multiple access in LTE and 5G networks," *IEEE Commun. Mag.*, vol. 55, no. 2, pp. 185–191, Feb. 2017.

[19] W. Liang, S. X. Ng, J. Shi, L. Li, and D. Wang, "Energy efficient transmission in underlay CR-NOMA networks enabled by reinforcement learning," *China Commun.*, vol. 17, no. 12, pp. 66–79, Dec. 2020.

[20] S. M. R. Islam, N. Avazov, O. A. Dobre, and K.-S. Kwak, "Power-domain non-orthogonal multiple access (NOMA) in 5G systems: Potentials and challenges," *IEEE Commun. Surveys Tuts.*, vol. 19, no. 2, pp. 721–742, 2nd Quart., 2017.

[21] Y. Wang, Z. Tian, and X. Cheng, "Enabling technologies for spectrum and energy efficient NOMA-MmWave-MaMIMO systems," *IEEE Wireless Commun.*, vol. 27, no. 5, pp. 53–59, Oct. 2020.

[22] A. S. D. Sena *et al.*, "What role do intelligent reflecting surfaces play in multi-antenna non-orthogonal multiple access?" *IEEE Wireless Commun.*, vol. 27, no. 5, pp. 24–31, Oct. 2020.

[23] M. Mohammadkarimi, M. A. Raza, and O. A. Dobre, "Signature-based nonorthogonal massive multiple access for future wireless networks: Uplink massive connectivity for machine-type communications," *IEEE Veh. Technol. Mag.*, vol. 13, no. 4, pp. 40–50, Dec. 2018.

[24] C. You, B. Zheng, and R. Zhang, "Wireless communication via double IRS: Channel estimation and passive beamforming designs," *IEEE Wireless Commun. Lett.*, vol. 10, no. 2, pp. 431–435, Feb. 2021.

[25] X. Yu, D. Xu, Y. Sun, D. W. K. Ng, and R. Schober, "Robust and secure wireless communications via intelligent reflecting surfaces," *IEEE J. Sel. Areas Commun.*, vol. 38, no. 11, pp. 2637–2652, Nov. 2020.

[26] M. Najafi, V. Jamali, R. Schober, and H. V. Poor, "Physics-based modeling and scalable optimization of large intelligent reflecting surfaces," *IEEE Trans. Commun.*, vol. 69, no. 4, pp. 2673–2691, Apr. 2021.

[27] R. Hadani and A. Monk, "OTFS: A new generation of modulation addressing the challenges of 5G," 2018, *arXiv:1802.02623*.

[28] P. Raviteja, Y. Hong, E. Viterbo, and E. Biglieri, "Practical pulse-shaping waveforms for reduced-cyclic-prefix OTFS," *IEEE Trans. Veh. Tech.*, vol. 68, no. 1, pp. 957–961, Jan. 2019.

[29] Z. Ding, "Harvesting devices' heterogeneous energy profiles and QoS requirements in IoT: WPT-NOMA vs BAC-NOMA," *IEEE Trans. Commun.*, vol. 69, no. 5, pp. 2837–2850, May 2021.

[30] Q. N. Le, A. Yadav, N.-P. Nguyen, O. A. Dobre, and R. Zhao, "Full-duplex non-orthogonal multiple access cooperative overlay spectrum-sharing networks with SWIPT," *IEEE Trans. Green Commun. Netw.*, vol. 5, no. 1, pp. 322–334, Mar. 2021.

[31] J. Tang *et al.*, "Decoupling or learning: Joint power splitting and allocation in MC-NOMA with SWIPT," *IEEE Trans. Commun.*, vol. 68, no. 9, pp. 5834–5848, Sep. 2020.

[32] Y. Saito, A. Benjebbour, Y. Kishiyama, and T. Nakamura, "System-level performance evaluation of downlink non-orthogonal multiple access (NOMA)," in *Proc. IEEE 24th Annu. Int. Symp. Pers., Indoor, Mobile Radio Commun. (PIMRC)*, London, U.K., Sep. 2013, pp. 611–615.

[33] Z. Ding, Z. Yang, P. Fan, and H. V. Poor, "On the performance of non-orthogonal multiple access in 5G systems with randomly deployed users," *IEEE Signal Process. Lett.*, vol. 21, no. 12, pp. 1501–1505, Dec. 2014.

[34] B. Zheng, Q. Wu, and R. Zhang, "Intelligent reflecting surface-assisted multiple access with user pairing: NOMA or OMA?" *IEEE Commun. Lett.*, vol. 24, no. 4, pp. 753–757, Apr. 2020.

[35] Z. Ding, R. Schober, and H. V. Poor, "On the impact of phase shifting designs on IRS-NOMA," *IEEE Wireless Commun. Lett.*, vol. 9, no. 10, pp. 1596–1600, Oct. 2020.

[36] Z. Ding and H. V. Poor, "A simple design of IRS-NOMA transmission," *IEEE Commun. Lett.*, vol. 24, no. 5, pp. 1119–1123, May 2020.

[37] M. Zeng, X. Li, G. Li, W. Hao, and O. A. Dobre, "Sum rate maximization for IRS-assisted uplink NOMA," *IEEE Commun. Lett.*, vol. 25, no. 1, pp. 234–238, Sep. 2021.

[38] Z. Chen, Z. Ding, P. Xu, and X. Dai, "Optimal precoding for a QoS optimization problem in two-user MISO-NOMA downlink," *IEEE Commun. Lett.*, vol. 20, no. 6, pp. 1263–1266, Jun. 2016.

[39] Z. Chen, Z. Ding, X. Dai, and G. K. Karagiannidis, "On the application of quasi-degradation to MISO-NOMA downlink," *IEEE Trans. Signal Process.*, vol. 64, no. 23, pp. 6174–6189, Dec. 2016.

[40] J. Zhu, Y. Huang, J. Wang, K. Navaie, and Z. Ding, "Power efficient IRS-assisted NOMA," *IEEE Trans. Commun.*, vol. 69, no. 2, pp. 900–913, Feb. 2021.

[41] Z. Ding, R. Schober, and H. V. Poor, "Unveiling the importance of SIC in NOMA systems—Part 1: State of the art and recent findings," *IEEE Commun. Lett.*, vol. 24, no. 11, pp. 2373–2377, Nov. 2020.

[42] Z. Ding, R. Schober, and H. V. Poor, "Unveiling the importance of SIC in NOMA systems—Part II: New results and future directions," *IEEE Commun. Lett.*, vol. 24, no. 11, pp. 2378–2382, Nov. 2020.

[43] Z. Ding, "NOMA beamforming in SDMA networks: Riding on existing beams or forming new ones?" 2022, *arXiv:2201.04082*.

[44] Q. Wu and R. Zhang, "Intelligent reflecting surface enhanced wireless network: Joint active and passive beamforming design," in *Proc. IEEE Global Commun. Conf. (GLOBECOM)*, Dec. 2018, pp. 1–6.

[45] Y. Guo, Z. Qin, Y. Liu, and N. Al-Dhahir, "Intelligent reflecting surface aided multiple access over fading channels," *IEEE Trans. Commun.*, vol. 69, no. 3, pp. 2015–2027, Mar. 2021.

[46] Q. Wu, X. Zhou, and R. Schober, "IRS-assisted wireless powered NOMA: Do we really need different phase shifts in DL and UL?" *IEEE Wireless Commun. Lett.*, vol. 10, no. 7, pp. 1493–1497, Jul. 2021.

[47] J. Zuo, Y. Liu, Z. Qin, and N. Al-Dhahir, "Resource allocation in intelligent reflecting surface assisted NOMA systems," *IEEE Trans. Commun.*, vol. 68, no. 11, pp. 7170–7183, Nov. 2020.

[48] X. Mu, Y. Liu, L. Guo, J. Lin, and R. Schober, "Joint deployment and multiple access design for intelligent reflecting surface assisted networks," *IEEE Trans. Wireless Commun.*, vol. 20, no. 10, pp. 6648–6664, Oct. 2021.

[49] X. Mu, Y. Liu, L. Guo, J. Lin, and N. Al-Dhahir, "Exploiting intelligent reflecting surfaces in NOMA networks: Joint beamforming optimization," *IEEE Trans. Wireless Commun.*, vol. 19, no. 10, pp. 6884–6898, Oct. 2020.

[50] J. Zuo, Y. Liu, E. Basar, and O. A. Dobre, "Intelligent reflecting surface enhanced millimeter-wave NOMA systems," *IEEE Commun. Lett.*, vol. 24, no. 11, pp. 2632–2636, Nov. 2020.

[51] P. Liu, Y. Li, W. Cheng, X. Gao, and X. Huang, "Intelligent reflecting surface aided NOMA for millimeter-wave massive MIMO with lens antenna array," *IEEE Trans. Veh. Technol.*, vol. 70, no. 5, pp. 4419–4434, May 2021.

[52] A. S. de Sena *et al.*, "IRS-assisted massive MIMO-NOMA networks: Exploiting wave polarization," *IEEE Trans. Wireless Commun.*, vol. 20, no. 11, pp. 7166–7183, Nov. 2021.

[53] S. Jiao, F. Fang, X. Zhou, and H. Zhang, "Joint beamforming and phase shift design in downlink UAV networks with IRS-assisted NOMA," *J. Commun. Inf. Netw.*, vol. 5, no. 2, pp. 138–149, Jun. 2020.

[54] X. Mu, Y. Liu, L. Guo, J. Lin, and H. V. Poor, "Intelligent reflecting surface enhanced multi-UAV NOMA networks," *IEEE J. Sel. Areas Commun.*, vol. 39, no. 10, pp. 3051–3066, Oct. 2021.

[55] M. Fu, Y. Zhou, and Y. Shi, "Intelligent reflecting surface for downlink non-orthogonal multiple access networks," in *Proc. IEEE Globecom Workshops (GC Wkshps)*, Dec. 2019, pp. 1–6.

[56] Y. Li, M. Jiang, Q. Zhang, and J. Qin, "Joint beamforming design in multi-cluster MISO NOMA reconfigurable intelligent surface-aided downlink communication networks," *IEEE Trans. Commun.*, vol. 69, no. 1, pp. 664–674, Jan. 2021.

[57] X. Xie, F. Fang, and Z. Ding, "Joint optimization of beamforming, phase-shifting and power allocation in a multi-cluster IRS-NOMA network," *IEEE Trans. Veh. Technol.*, vol. 70, no. 8, pp. 7705–7717, Aug. 2021.

[58] F. Fang, Y. Xu, Q.-V. Pham, and Z. Ding, "Energy-efficient design of IRS-NOMA networks," *IEEE Trans. Veh. Technol.*, vol. 69, no. 11, pp. 14088–14092, Nov. 2020.

[59] F. Fang, H. Zhang, J. Cheng, S. Roy, and V. C. M. Leung, "Joint user scheduling and power allocation optimization for energy-efficient NOMA systems with imperfect CSI," *IEEE J. Sel. Areas Commun.*, vol. 35, no. 12, pp. 2874–2885, Dec. 2017.

[60] F. Fang, H. Zhang, J. Cheng, and V. C. M. Leung, "Energy-efficient resource allocation for downlink non-orthogonal multiple access network," *IEEE Trans. Commun.*, vol. 64, no. 9, pp. 3722–3732, Sep. 2016.

[61] A. Taha, M. Alrabeiah, and A. Alkhateeb, "Enabling large intelligent surfaces with compressive sensing and deep learning," *IEEE Access*, vol. 9, pp. 44304–44321, 2021.

[62] C. Huang, G. C. Alexandropoulos, C. Yuen, and M. Debbah, "Indoor signal focusing with deep learning designed reconfigurable intelligent surfaces," in *Proc. IEEE 20th Int. Workshop Signal Process. Adv. Wireless Commun. (SPAWC)*, Cannes, France, Jul. 2019, pp. 1–5.

[63] H. Li, F. Fang, and Z. Ding, "DRL-assisted resource allocation for NOMA-MEC offloading with hybrid SIC," *Entropy*, vol. 23, no. 5, p. 613, May 2021.

[64] X. Liu, Y. Liu, Y. Chen, and H. V. Poor, "RIS enhanced massive non-orthogonal multiple access networks: Deployment and passive beamforming design," *IEEE J. Sel. Areas Commun.*, vol. 39, no. 4, pp. 1057–1071, Apr. 2021.

[65] X. Gao, Y. Liu, X. Liu, and L. Song, "Machine learning empowered resource allocation in IRS aided MISO-NOMA networks," *IEEE Trans. Wireless Commun.*, vol. 21, no. 5, pp. 3478–3492, May 2022.

[66] Z. Yang, Y. Liu, Y. Chen, and N. Al-Dhahir, "Machine learning for user partitioning and phase shifters design in RIS-aided NOMA networks," *IEEE Trans. Commun.*, vol. 69, no. 11, pp. 7414–7428, Nov. 2021.

[67] M. Shehab, B. S. Ciftler, T. Khattab, M. Abdallah, and D. Trinchero, "Deep reinforcement learning powered IRS-assisted downlink NOMA," 2021, *arXiv:2104.01414*.

[68] Y. Guo, F. Fang, D. Cai, and Z. Ding, "Energy-efficient design for a NOMA assisted STAR-RIS network with deep reinforcement learning," 2021, *arXiv:2111.15464*.

[69] W. Ni, Y. Liu, Z. Yang, H. Tian, and X. Shen, "Federated learning in multi-RIS aided systems," *IEEE Internet Things J.*, early access, Nov. 24, 2021, doi: 10.1109/JIOT.2021.3130444.

[70] L. Lv, F. Zhou, J. Chen, and N. Al-Dhahir, "Secure cooperative communications with an untrusted relay: A NOMA-inspired jamming and relaying approach," *IEEE Trans. Inf. Forensics Security*, vol. 14, no. 12, pp. 3191–3205, Dec. 2019.

[71] L. Lv, H. Jiang, Z. Ding, Q. Ye, N. Al-Dhahir, and J. Chen, "Secure non-orthogonal multiple access: An interference engineering perspective," *IEEE Netw.*, vol. 35, no. 4, pp. 278–285, Jul. 2021.

[72] L. Lv, Q. Wu, Z. Li, Z. Ding, N. Al-Dhahir, and J. Chen, "Covert communication in intelligent reflecting surface-assisted NOMA systems: Design, analysis, and optimization," *IEEE Trans. Wireless Commun.*, vol. 21, no. 3, pp. 1735–1750, Mar. 2022.

[73] L. Lv, H. Jiang, Z. Ding, L. Yang, and J. Chen, "Secrecy-enhancing design for cooperative downlink and uplink NOMA with an untrusted relay," *IEEE Trans. Commun.*, vol. 68, no. 3, pp. 1698–1715, Mar. 2020.

[74] M. Cui, G. Zhang, and R. Zhang, "Secure wireless communication via intelligent reflecting surface," *IEEE Wireless Commun. Lett.*, vol. 8, no. 5, pp. 1410–1414, Oct. 2019.

[75] Z. Chu, W. Hao, P. Xiao, and J. Shi, "Intelligent reflecting surface aided multi-antenna secure transmission," *IEEE Wireless Commun. Lett.*, vol. 9, no. 1, pp. 108–112, Jan. 2020.

[76] L. Dong and H.-M. Wang, "Enhancing secure MIMO transmission via intelligent reflecting surface," *IEEE Trans. Wireless Commun.*, vol. 19, no. 11, pp. 7543–7556, Nov. 2020.

[77] S. Yan, X. Zhou, D. W. K. Ng, J. Yuan, and N. Al-Dhahir, "Intelligent reflecting surface for wireless communication security and privacy," 2021, *arXiv:2103.16696*.

[78] Z. Zhang, L. Lv, Q. Wu, H. Deng, and J. Chen, "Robust and secure communications in intelligent reflecting surface assisted NOMA networks," *IEEE Commun. Lett.*, vol. 25, no. 3, pp. 739–743, Mar. 2021.

[79] Z. Zhang, J. Chen, Q. Wu, Y. Liu, L. Lv, and X. Su, "Securing NOMA networks by exploiting intelligent reflecting surface," *IEEE Trans. Commun.*, vol. 70, no. 2, pp. 1096–1111, Feb. 2022.

[80] L. Lv, Q. Wu, Z. Li, N. Al-Dhahir, and J. Chen, "Secure two-way communications via intelligent reflecting surfaces," *IEEE Commun. Lett.*, vol. 25, no. 3, pp. 744–748, Mar. 2021.

[81] X. Guan, Q. Wu, and R. Zhang, "Intelligent reflecting surface assisted secrecy communication: Is artificial noise helpful or not?" *IEEE Wireless Commun. Lett.*, vol. 9, no. 6, pp. 778–782, Jun. 2020.

[82] H.-M. Wang, J. Bai, and L. Dong, "Intelligent reflecting surfaces assisted secure transmission without eavesdropper's CSI," *IEEE Signal Process. Lett.*, vol. 27, pp. 1300–1304, 2020.

[83] S. Xu, J. Liu, and Y. Cao, "Intelligent reflecting surface empowered physical-layer security: Signal cancellation or jamming?" *IEEE Internet Things J.*, vol. 9, no. 2, pp. 1265–1275, Jan. 2022.

[84] L. Tao, W. Yang, S. Yan, D. Wu, X. Guan, and D. Chen, "Covert communication in downlink NOMA systems with random transmit power," *IEEE Wireless Commun. Lett.*, vol. 9, no. 11, pp. 2000–2004, Nov. 2020.

[85] X. Lu, E. Hossain, T. Shafique, S. Feng, H. Jiang, and D. Niyato, "Intelligent reflecting surface (IRS)-enabled covert communications in wireless networks," *IEEE Netw.*, vol. 34, no. 5, pp. 148–155, Sep./Oct. 2020.

[86] L. Lv, Q. Wu, Z. Li, Z. Ding, N. Al-Dhahir, and J. Chen, "Achieving covert communication by IRS-NOMA," in *Proc. IEEE/CIC Int. Conf. Commun. China (ICCC)*, Jul. 2021, pp. 421–426.

[87] L. Lv, Z. Ding, J. Chen, and N. Al-Dhahir, "Design of secure NOMA against full-duplex proactive eavesdropping," *IEEE Wireless Commun. Lett.*, vol. 8, no. 4, pp. 1090–1094, Aug. 2019.

[88] Q. Wu, S. Zhang, B. Zheng, C. You, and R. Zhang, "Intelligent reflecting surface-aided wireless communications: A tutorial," *IEEE Trans. Commun.*, vol. 69, no. 5, pp. 3313–3351, May 2021.

[89] A. Taha, M. Alrabeiah, and A. Alkhateeb, "Deep learning for large intelligent surfaces in millimeter wave and massive MIMO systems," in *Proc. IEEE Global Commun. Conf. (GLOBECOM)*, Dec. 2019, pp. 1–6.

[90] G. C. Alexandropoulos and E. Vlachos, "A hardware architecture for reconfigurable intelligent surfaces with minimal active elements for explicit channel estimation," in *Proc. IEEE Int. Conf. Acoust., Speech Signal Process. (ICASSP)*, May 2020, pp. 9175–9179.

[91] D. Mishra and H. Johansson, "Channel estimation and low-complexity beamforming design for passive intelligent surface assisted MISO wireless energy transfer," in *Proc. IEEE Int. Conf. Acoust., Speech Signal Process. (ICASSP)*, May 2019, pp. 4659–4663.

[92] Y. Yang, B. Zheng, S. Zhang, and R. Zhang, "Intelligent reflecting surface meets OFDM: Protocol design and rate maximization," *IEEE Trans. Commun.*, vol. 68, no. 7, pp. 4522–4535, Jul. 2020.

[93] B. Zheng and R. Zhang, "Intelligent reflecting surface-enhanced OFDM: Channel estimation and reflection optimization," *IEEE Wireless Commun. Lett.*, vol. 9, no. 4, pp. 518–522, Apr. 2020.

[94] Z.-Q. He and X. Yuan, "Cascaded channel estimation for large intelligent metasurface assisted massive MIMO," *IEEE Wireless Commun. Lett.*, vol. 9, no. 2, pp. 210–214, Feb. 2020.

[95] H. Liu, X. Yuan, and Y.-J.-A. Zhang, "Matrix-calibration-based cascaded channel estimation for reconfigurable intelligent surface assisted multiuser MIMO," *IEEE J. Sel. Areas Commun.*, vol. 38, no. 11, pp. 2621–2636, Nov. 2020.

[96] C. Hu, L. Dai, S. Han, and X. Wang, "Two-timescale channel estimation for reconfigurable intelligent surface aided wireless communications," *IEEE Trans. Commun.*, vol. 69, no. 11, pp. 7736–7747, Nov. 2021.

[97] G. Zhou, C. Pan, H. Ren, K. Wang, and A. Nallanathan, "A framework of robust transmission design for IRS-aided MISO communications with imperfect cascaded channels," *IEEE Trans. Signal Process.*, vol. 68, pp. 5092–5106, 2020.

[98] G. Zhou, C. Pan, H. Ren, K. Wang, M. Di Renzo, and A. Nallanathan, "Robust beamforming design for intelligent reflecting surface aided MISO

communication systems," *IEEE Wireless Commun. Lett.*, vol. 9, no. 10, pp. 1658–1662, Oct. 2020.
[99] S. Hong, C. Pan, H. Ren, K. Wang, K. K. Chai, and A. Nallanathan, "Robust transmission design for intelligent reflecting surface-aided secure communication systems with imperfect cascaded CSI," *IEEE Trans. Wireless Commun.*, vol. 20, no. 4, pp. 2487–2501, Apr. 2021.
[100] F. Fang, K. Wang, Z. Ding, and V. C. M. Leung, "Energy-efficient resource allocation for NOMA-MEC networks with imperfect CSI," *IEEE Trans. Commun.*, vol. 69, no. 5, pp. 3436–3449, May 2021.
[101] M. M. Zhao, Q. Wu, M. J. Zhao, and R. Zhang, "Exploiting amplitude control in intelligent reflecting surface aided wireless communication with imperfect CSI," *IEEE Trans. Commun.*, vol. 69, no. 6, pp. 4216–4231, Jun. 2021.
[102] K. Zhi, C. Pan, H. Ren, and K. Wang, "Statistical CSI-based design for reconfigurable intelligent surface-aided massive MIMO systems with direct links," *IEEE Wireless Commun. Lett.*, vol. 10, no. 5, pp. 1128–1132, May 2021.
[103] Z. Peng, T. Li, C. Pan, H. Ren, W. Xu, and M. D. Renzo, "Analysis and optimization for RIS-aided multi-pair communications relying on statistical CSI," *IEEE Trans. Veh. Technol.*, vol. 70, no. 4, pp. 3897–3901, Apr. 2021.
[104] L. You *et al.*, "Reconfigurable intelligent surfaces-assisted multiuser MIMO uplink transmission with partial CSI," *IEEE Trans. Wireless Commun.*, vol. 20, no. 9, pp. 5613–5627, Sep. 2021.
[105] J. Dai, Y. Wang, C. Pan, K. Zhi, H. Ren, and K. Wang, "Reconfigurable intelligent surface aided massive MIMO systems with low-resolution DACs," *IEEE Commun. Lett.*, vol. 25, no. 9, pp. 3124–3128, Sep. 2021.
[106] A. Papazafeiropoulos, C. Pan, P. Kourtessis, S. Chatzinotas, and J. M. Senior, "Intelligent reflecting surface-assisted MU-MISO systems with imperfect hardware: Channel estimation and beamforming design," *IEEE Trans. Wireless Commun.*, vol. 21, no. 3, pp. 2077–2092, Mar. 2022.
[107] J. Dai, F. Zhu, C. Pan, H. Ren, and K. Wang, "Statistical CSI-based transmission design for reconfigurable intelligent surface-aided massive MIMO systems with hardware impairments," *IEEE Wireless Commun. Lett.*, vol. 11, no. 1, pp. 38–42, Jan. 2022.
[108] K. Zhi *et al.*, "Two-timescale design for reconfigurable intelligent surface-aided massive MIMO systems with imperfect CSI," 2021, *arXiv:2108.07622*.
[109] M.-M. Zhao, A. Liu, Y. Wan, and R. Zhang, "Two-timescale beamforming optimization for intelligent reflecting surface aided multiuser communication with QoS constraints," *IEEE Trans. Wireless Commun.*, vol. 20, no. 9, pp. 6179–6194, Sep. 2021.
[110] M.-M. Zhao, Q. Wu, M.-J. Zhao, and R. Zhang, "Intelligent reflecting surface enhanced wireless networks: Two-timescale beamforming optimization," *IEEE Trans. Wireless Commun.*, vol. 20, no. 1, pp. 2–17, Jan. 2021.
[111] X. Chen, R. Jia, and D. W. K. Ng, "On the design of massive non-orthogonal multiple access with imperfect successive interference cancellation," *IEEE Trans. Commun.*, vol. 67, no. 3, pp. 2539–2551, Mar. 2019.
[112] Y. Liu, X. Mu, X. Liu, M. Di Renzo, Z. Ding, and R. Schober, "Reconfigurable intelligent surface (RIS) aided multi-user networks: Interplay between NOMA and RIS," 2020, *arXiv:2011.13336*.
[113] Z. Ding, P. Fan, and H. V. Poor, "Impact of user pairing on 5G non-orthogonal multiple-access downlink transmissions," *IEEE Trans. Veh. Technol.*, vol. 65, no. 8, pp. 6010–6023, Aug. 2016.
[114] S. Zhang and R. Zhang, "Intelligent reflecting surface aided multi-user communication: Capacity region and deployment strategy," *IEEE Trans. Commun.*, vol. 69, no. 9, pp. 5790–5806, Sep. 2021.
[115] C. You, B. Zheng, W. Mei, and R. Zhang, "How to deploy intelligent reflecting surfaces in wireless network: BS-side, user-side, or both sides?" 2020, *arXiv:2012.03403*.
[116] W. Chen, L. Bai, W. Tang, S. Jin, W. X. Jiang, and T. J. Cui, "Angle-dependent phase shifter model for reconfigurable intelligent surfaces: Does the angle-reciprocity hold?" *IEEE Commun. Lett.*, vol. 24, no. 9, pp. 2060–2064, Sep. 2020.
[117] N.-N. Dao *et al.*, "Survey on aerial radio access networks: Toward a comprehensive 6G access infrastructure," *IEEE Commun. Surveys Tuts.*, vol. 23, no. 2, pp. 1193–1225, 2nd Quart., 2021.
[118] Q. Wu, Y. Zeng, and R. Zhang, "Joint trajectory and communication design for multi-UAV enabled wireless networks," *IEEE Trans. Wireless Commun.*, vol. 17, no. 3, pp. 2109–2121, Mar. 2018.
[119] Y. Zeng, Q. Wu, and R. Zhang, "Accessing from the sky: A tutorial on UAV communications for 5G and beyond," *Proc. IEEE*, vol. 107, no. 12, pp. 2327–2375, Dec. 2019.
[120] S. Li, B. Duo, X. Yuan, Y.-C. Liang, and M. Di Renzo, "Reconfigurable intelligent surface assisted UAV communication: Joint trajectory design and passive beamforming," *IEEE Wireless Commun. Lett.*, vol. 9, no. 5, pp. 716–720, Jan. 2020.
[121] M. Hua, L. Yang, Q. Wu, C. Pan, C. Li, and A. L. Swindlehurst, "UAV-assisted intelligent reflecting surface symbiotic radio system," *IEEE Trans. Wireless Commun.*, vol. 20, no. 9, pp. 5769–5785, Sep. 2021.
[122] Y. Pan, K. Wang, C. Pan, H. Zhu, and J. Wang, "UAV-assisted and intelligent reflecting surfaces-supported terahertz communications," *IEEE Wireless Commun. Lett.*, vol. 10, no. 6, pp. 1256–1260, Jun. 2021.
[123] H. Lu, Y. Zeng, S. Jin, and R. Zhang, "Aerial intelligent reflecting surface: Joint placement and passive beamforming design with 3D beam flattening," *IEEE Trans. Wireless Commun.*, vol. 20, no. 7, pp. 4128–4143, Jul. 2021.
[124] Y. Liu, Z. Qin, Y. Cai, Y. Gao, G. Y. Li, and A. Nallanathan, "UAV communications based on non-orthogonal multiple access," *IEEE Wireless Commun.*, vol. 26, no. 1, pp. 52–57, Feb. 2019.
[125] X. Liu, Y. Liu, and Y. Chen, "Machine learning empowered trajectory and passive beamforming design in UAV-RIS wireless networks," *IEEE J. Sel. Areas Commun.*, vol. 39, no. 7, pp. 2042–2055, Jul. 2021.
[126] J. Zuo, Y. Liu, Z. Ding, L. Song, and H. V. Poor, "Joint design for simultaneously transmitting and reflecting (STAR) RIS assisted NOMA systems," 2021, *arXiv:2106.03001*.
[127] *Starlink*. Accessed: 2022. [Online]. Available: https://www.starlink.com
[128] *Airbus*. Accessed: 2022. [Online]. Available: https://www.airbus.com/defence/uav/zephyr.html
[129] *Thales*. Accessed: 2022. [Online]. Available: https://www.thalesgroup.com/en/worldwide/space/news/whats/stratobus
[130] *HAPS Mobile*. Accessed: 2022. [Online]. Available: https://www.hapsmobile.com/en/
[131] K. Tekbıyık, G. K. Kurt, A. R. Ekti, and H. Yanikomeroglu, "Reconfigurable intelligent surfaces in action for non-terrestrial networks," 2020, *arXiv:2012.00968*.
[132] K. Tekbiyik, G. K. Kurt, and H. Yanikomeroglu, "Energy-efficient RIS-assisted satellites for IoT networks," *IEEE Internet Things J.*, early access, Sep. 16, 2021, doi: 10.1109/JIOT.2021.3112881.
[133] Y. Mao, C. You, J. Zhang, K. Huang, and K. B. Letaief, "A survey on mobile edge computing: The communication perspective," *IEEE Commun. Surveys Tuts.*, vol. 19, no. 4, pp. 2322–2358, 4th Quart., 2017.
[134] C. You, K. Huang, H. Chae, and B.-H. Kim, "Energy-efficient resource allocation for mobile-edge computation offloading," *IEEE Trans. Wireless Commun.*, vol. 16, no. 3, pp. 1397–1411, Mar. 2017.
[135] Z. Ding, P. Fan, and H. V. Poor, "Impact of non-orthogonal multiple access on the offloading of mobile edge computing," *IEEE Trans. Commun.*, vol. 67, no. 1, pp. 375–390, Jan. 2019.
[136] Z. Yang, C. Pan, J. Hou, and M. Shikh-Bahaei, "Efficient resource allocation for mobile-edge computing networks with NOMA: Completion time and energy minimization," *IEEE Trans. Commun.*, vol. 67, no. 11, pp. 7771–7784, Nov. 2019.
[137] Z. Ding, J. Xu, O. A. Dobre, and V. Poor, "Joint power and time allocation for NOMA-MEC offloading," *IEEE Trans. Veh. Technol.*, vol. 68, no. 6, pp. 6207–6211, Mar. 2019.
[138] K. Wang, F. Fang, D. B. D. Costa, and Z. Ding, "Sub-channel scheduling, task assignment, and power allocation for OMA-based and NOMA-based MEC systems," *IEEE Trans. Commun.*, vol. 69, no. 4, pp. 2692–2708, Apr. 2021.
[139] T. Bai, C. Pan, Y. Deng, M. Elkashlan, A. Nallanathan, and L. Hanzo, "Latency minimization for intelligent reflecting surface aided mobile edge computing," *IEEE J. Sel. Areas Commun.*, vol. 38, no. 11, pp. 2666–2682, Nov. 2020.
[140] Y. Cao and T. Lv, "Intelligent reflecting surface enhanced resilient design for MEC offloading over millimeter wave links," 2019, *arXiv:1912.06361*.
[141] T. Jiang and Y. Shi, "Over-the-air computation via intelligent reflecting surfaces," in *Proc. IEEE Global Commun. Conf. (GLOBECOM)*, Dec. 2019, pp. 1–6.
[142] F. Zhou, C. You, and R. Zhang, "Delay-optimal scheduling for IRS-aided mobile edge computing," *IEEE Wireless Commun. Lett.*, vol. 10, no. 4, pp. 740–744, Dec. 2021.
[143] Z. Li *et al.*, "Energy efficient reconfigurable intelligent surface enabled mobile edge computing networks with NOMA," *IEEE Trans. Cognit. Commun. Netw.*, vol. 7, no. 2, pp. 427–440, Jun. 2021.
[144] Y. Zeng, B. Clerckx, and R. Zhang, "Communications and signals design for wireless power transmission," *IEEE Trans. Commun.*, vol. 65, no. 5, pp. 2264–2290, May 2017.
[145] Z. Ding *et al.*, "Application of smart antenna technologies in simultaneous wireless information and power transfer," *IEEE Commun. Mag.*, vol. 53, no. 4, pp. 86–93, Apr. 2015.
[146] B. Lyu, P. Ramezani, D. T. Hoang, S. Gong, Z. Yang, and A. Jamalipour, "Optimized energy and information relaying in self-sustainable IRS-empowered WPCN," *IEEE Trans. Commun.*, vol. 69, no. 1, pp. 619–633, Jan. 2021.
[147] Y. Zheng, S. Bi, Y.-J.-A. Zhang, X. Lin, and H. Wang, "Joint beamforming and power control for throughput maximization in IRS-assisted MISO WPCNs," *IEEE Internet Things J.*, vol. 8, no. 10, pp. 8399–8410, May 2021.
[148] Q. Wu and R. Zhang, "Joint active and passive beamforming optimization for intelligent reflecting surface assisted SWIPT under QoS constraints," *IEEE J. Sel. Areas Commun.*, vol. 38, no. 8, pp. 1735–1748, Aug. 2020.
[149] Q. Wu and R. Zhang, "Weighted sum power maximization for intelligent reflecting surface aided SWIPT," *IEEE Wireless Commun. Lett.*, vol. 9, no. 5, pp. 586–590, May 2020.
[150] C. Pan *et al.*, "Intelligent reflecting surface enhanced MIMO broadcasting for simultaneous wireless information and power transfer," *IEEE J. Sel. Areas Commun.*, vol. 38, no. 8, pp. 1719–1734, Aug. 2020.
[151] P. D. Diamantoulakis, K. N. Pappi, Z. Ding, and G. K. Karagiannidis, "Wireless-powered communications with non-orthogonal multiple access," *IEEE Trans. Wireless Commun.*, vol. 15, no. 12, pp. 8422–8436, Dec. 2016.
[152] Y. Liu, Z. Ding, M. Elkashlan, and H. V. Poor, "Cooperative non-orthogonal multiple access with simultaneous wireless information and power transfer," *IEEE J. Sel. Areas Commun.*, vol. 34, no. 4, pp. 938–953, Apr. 2016.
[153] D. Zhang, Q. Wu, M. Cui, G. Zhang, and D. Niyato, "Throughput maximization for IRS-assisted wireless powered hybrid NOMA and TDMA," *IEEE Wireless Commun. Lett.*, vol. 10, no. 9, pp. 1944–1948, Sep. 2021.
[154] Z. Li, W. Chen, Q. Wu, K. Wang, and J. Li, "Joint

beamforming design and power splitting optimization in IRS-assisted SWIPT NOMA networks," *IEEE Trans. Wireless Commun.*, vol. 21, no. 3, pp. 2019–2033, Mar. 2022.
[155] H.-J. Song and T. Nagatsuma, "Present and future of terahertz communications," *IEEE Trans. THz Sci. Technol.*, vol. 1, no. 1, pp. 256–263, Sep. 2011.
[156] I. F. Akyildiz, J. M. Jornet, and C. Han, "Terahertz band: Next frontier for wireless communications," *Phys. Commun.*, vol. 12, no. 7, pp. 16–32, Jan. 2014.
[157] H. Burchardt, N. Serafimovski, D. Tsonev, S. Videv, and H. Haas, "VLC: Beyond point-to-point communication," *IEEE Commun. Mag.*, vol. 52, no. 7, pp. 98–105, Jul. 2014.
[158] N. Olson, J. G. Andrews, and R. W. Heath, Jr., "Coverage in terahertz cellular networks with imperfect beam alignment," in *Proc. IEEE Global Commun. Conf. (GLOBECOM)*, Madrid, Spain, Dec. 2021, pp. 1–6.
[159] H. G. Sandalidis, T. A. Tsiftsis, G. K. Karagiannidis, and M. Uysal, "BER performance of FSO links over strong atmospheric turbulence channels with pointing errors," *IEEE Commun. Lett.*, vol. 12, no. 1, pp. 44–46, Jan. 2008.
[160] Z. Ding, P. Fan, and H. V. Poor, "Random beamforming in millimeter-wave NOMA networks," *IEEE Access*, vol. 5, pp. 7667–7681, 2017.

ABOUT THE AUTHORS

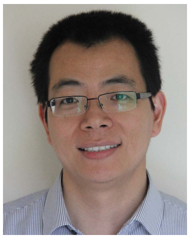

Zhiguo Ding (Fellow, IEEE) received the B.Eng. degree from the Beijing University of Posts and Telecommunications, Beijing, China, in 2000, and the Ph.D. degree from Imperial College London, London, U.K., in 2005.

Since April 2018, he has been with The University of Manchester, Manchester, U.K., as a Professor in communications. From October 2012 to September 2022, he has been an Academic Visitor with Princeton University, Princeton, NJ, USA. His research interests are 5G networks, game theory, cooperative and energy-harvesting networks, and statistical signal processing.

Dr. Ding recently received the EU Marie Curie Fellowship for the term 2012–2014, the Top IEEE TVT Editor in 2017, the IEEE Heinrich Hertz Award in 2018, the IEEE Jack Neubauer Memorial Award in 2018, the IEEE Best Signal Processing Letter Award in 2018, the Friedrich Wilhelm Bessel Research Award in 2020, and the IEEE SPCC Technical Recognition Award in 2021. He is serving as an Area Editor for the IEEE OPEN JOURNAL OF THE COMMUNICATIONS SOCIETY and an Editor for IEEE TRANSACTIONS ON VEHICULAR TECHNOLOGY and IEEE WIRELESS COMMUNICATION LETTERS, IEEE TRANSACTIONS ON COMMUNICATIONS, and IEEE COMMUNICATION LETTERS from 2013 to 2016. He is a Distinguished Lecturer of IEEE ComSoc and a Web of Science Highly Cited Researcher in two categories in 2021.

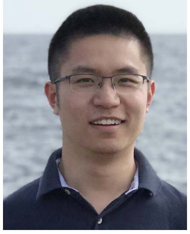

Lu Lv (Member, IEEE) received the Ph.D. degree from Xidian University, Xi'an, China, in 2018.

From 2016 to 2018, he was an Academic Visitor with Lancaster University, Lancaster, U.K., and the University of Alberta, Edmonton, AB, Canada. In 2019, he was a Postdoctoral Fellow with Dalhousie University, Halifax, NS, Canada. He is currently an Associate Professor with the State Key Laboratory of Integrated Services Networks, Xidian University. His research interests include nonorthogonal multiple access, physical layer security, intelligent reflecting surface, and covert communications.

Dr. Lv was a recipient of the Outstanding Ph.D. Thesis Award of Shaanxi Province in 2020, the Exemplary Reviewer Certificate for the IEEE TRANSACTIONS ON COMMUNICATIONS from 2018 to 2020 and the IEEE ICCC Best Paper Award in 2021. He serves as an Associate Editor for IEEE INTERNET OF THINGS, AD HOC AND SENSOR NETWORKS TECHNICAL COMMITTEE NEWSLETTER and *Frontiers in Computer Science*.

Fang Fang (Member, IEEE) received the Ph.D. degree in electrical engineering from The University of British Columbia (UBC), Kelowna, BC, Canada, in 2017.

From 2018 to 2020, she was a Research Associate with the Department of Electrical and Electronic Engineering, The University of Manchester, Manchester, U.K. She is currently an Assistant Professor with the Department of Electrical and Computer Engineering and the Department of Computer Science, Western University, London, ON, Canada. Prior to joining Western University, she was an Assistant Professor with the Department of Engineering, Durham University, Durham, U.K., from 2020 to 2022. Her current research interests include machine learning for intelligent wireless communications, nonorthogonal multiple access (NOMA), intelligent reflecting surface (IRS), multiaccess edge computing (MEC), machine learning for intelligent communications, blockchain, and edge artificial intelligence (AI).

Dr. Fang has been serving as a Technical Program Committee (TPC) Member for IEEE flagship conferences, e.g., IEEE Global Communications Conference (GLOBECOM), IEEE International Conference on Communications (ICC), and IEEE Vehicular Technology Conference (VTC). She received the Exemplary Reviewer Certificates of the IEEE TRANSACTIONS ON COMMUNICATIONS in 2017 and 2022. She is also an Associate Editor of IEEE OPEN JOURNAL OF THE COMMUNICATIONS SOCIETY.

Octavia A. Dobre (Fellow, IEEE) received the Dipl.Ing. and Ph.D. degrees from the Polytechnic Institute of Bucharest, Bucharest, Romania, in 1991 and 2000, respectively.

From 2002 to 2005, she was with the New Jersey Institute of Technology, Newark, NJ, USA. In 2005, she joined Memorial University, St. John's, NL, Canada, where she is currently a Professor and the Research Chair. She was a Visiting Professor with the Massachusetts Institute of Technology, Cambridge, MA, USA, and the Université de Bretagne Occidentale, Brest, France. Her research interests encompass wireless, optical, and underwater communication technologies. She has (co)authored over 400 refereed articles in these areas.

Dr. Dobre is a Fellow of the Engineering Institute of Canada and the Canadian Academy of Engineering. She received Best Paper Awards at various conferences, including IEEE International Conference on Communications (ICC), IEEE Global Communications Conference (GLOBECOM), IEEE Wireless Communications and Networking Conference (WCNC), and IEEE International Symposium on Personal, Indoor and Mobile Radio Communications (PIMRC). She served as a general chair, a technical program co-chair, a tutorial co-chair, and a technical co-chair for symposia at numerous conferences. She was a Fulbright Scholar, a Royal Society Scholar, and a Distinguished Lecturer of the IEEE Communications Society. She was the Editor-in-Chief of the IEEE COMMUNICATIONS LETTERS and a senior editor, an editor, and a guest editor for various prestigious journals and magazines. She serves as the Editor-in-Chief (EiC) for the IEEE OPEN JOURNAL OF THE COMMUNICATIONS SOCIETY.

George K. Karagiannidis (Fellow, IEEE) received the University Diploma (five years) and Ph.D. degrees in electrical and computer engineering from the University of Patras, Patras, Greece, in 1987 and 1999, respectively.

He is currently a Professor with the Department of Electrical and Computer Engineering and Head of the Wireless Communications and Information Processing (WCIP) Group, Aristotle University of Thessaloniki, Thessaloniki, Greece. He is also an Honorary Professor at South West Jiaotong University, Chengdu, China. His research interests are in the broad area of digital communications systems and signal processing.

Dr. Karagiannidis received the 2021 IEEE Communications Society Radio Communications Committee Technical Recognition Award and the 2018 Signal Processing and Communications Electronics Technical Recognition Award of the IEEE Communications Society. He serves as the Associate Editor-in-Chief for IEEE OPEN JOURNAL OF COMMUNICATIONS SOCIETY. He is one of the highly cited authors across all areas of electrical engineering, recognized from Clarivate Analytics as Web-of-Science Highly-Cited Researcher from 2015 to 2021.

Naofal Al-Dhahir (Fellow, IEEE) received the Ph.D. degree from Stanford University, Stanford, CA, USA, in 1994.

He is currently an Erik Jonsson Distinguished Professor and the Associate Head of the Department of Electrical and Computer Engineering, The University of Texas at Dallas, Richardson, TX, USA. He was a Principal Member of Technical Staff at the GE Research Center, New York, and the AT&T Shannon Laboratory, New Jersey, from 1994 to 2003. He is the co-inventor of 43 issued patents and the coauthor of about 500 articles. He was a co-recipient of five IEEE best paper awards.

Dr. Al-Dhahir is a Fellow of the National Academy of Inventors. He received the 2019 IEEE SPCC Technical Recognition Award and the 2021 Qualcomm Faculty Award. He served as the Editor-in-Chief for IEEE TRANSACTIONS ON COMMUNICATIONS from January 2016 to December 2019.

Robert Schober (Fellow, IEEE) received the Diplom (Univ.) and the Ph.D. degrees in electrical engineering from Friedrich-Alexander University of Erlangen-Nuremberg (FAU), Erlangen, Germany, in 1997 and 2000, respectively.

From 2002 to 2011, he was a Professor and the Canada Research Chair at The University of British Columbia (UBC), Vancouver, BC, Canada. Since January 2012, he has been an Alexander von Humboldt Professor and the Chair for Digital Communication at FAU. His research interests fall into the broad areas of communication theory, wireless and molecular communications, and statistical signal processing.

Dr. Schober is a Fellow of the Canadian Academy of Engineering and the Engineering Institute of Canada and a member of the German National Academy of Science and Engineering. He serves as a member of the Editorial Board of the PROCEEDINGS OF THE IEEE, a Member at Large of the ComSoc Board of Governors, and a ComSoc Treasurer. He received several awards for his work, including the 2002 Heinz Maier-Leibnitz Award of the German Science Foundation (DFG), the 2004 Innovations Award of the Vodafone Foundation for Research in Mobile Communications, the 2006 UBC Killam Research Prize, the 2007 Wilhelm Friedrich Bessel Research Award of the Alexander von Humboldt Foundation, the 2008 Charles McDowell Award for Excellence in Research from UBC, the 2011 Alexander von Humboldt Professorship, the 2012 NSERC E. W. R. Stacie Fellowship, the 2017 Wireless Communications Recognition Award by the IEEE Wireless Communications Technical Committee, and the 2021 ACM NanoCom Milestone Award for "fundamental contributions to the modeling, design, and analysis of molecular communication systems." Since 2017, he has been listed as a Highly Cited Researcher by the Web of Science. He served as the Editor-in-Chief for the IEEE TRANSACTIONS ON COMMUNICATIONS from 2012 to 2015 and VP Publications of the IEEE Communication Society (ComSoc) in 2020 and 2021.

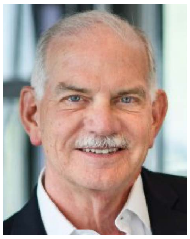

H. Vincent Poor (Life Fellow, IEEE) received the Ph.D. degree in electrical engineering and computer sciences (EECS) from Princeton University, Princeton, NJ, USA, in 1977.

From 1977 until 1990, he was on the faculty of the University of Illinois at Urbana–Champaign, Urbana, IL, USA. Since 1990, he has been on the faculty at Princeton, where he is currently the Michael Henry Strater University Professor. From 2006 to 2016, he was the Dean of Princeton's School of Engineering and Applied Science. He has also held visiting appointments at several other universities, including most recently at Berkeley and Cambridge. His research interests are in the areas of information theory, machine learning, and network science, and their applications in wireless networks, energy systems, and related fields. Among his publications in these areas is the forthcoming book *Machine Learning and Wireless Communications* (Cambridge University Press).

Dr. Poor is a member of the National Academy of Engineering and the National Academy of Sciences and is a foreign member of the Chinese Academy of Sciences, the Royal Society, and other national and international academies. He received the IEEE Alexander Graham Bell Medal in 2017.